

10163
NACA TN 3809

TECH LIBRARY KAFB, NM



0066769

NATIONAL ADVISORY COMMITTEE FOR AERONAUTICS

TECHNICAL NOTE 3809

A METHOD FOR CALCULATION OF FREE-SPACE SOUND PRESSURES
NEAR A PROPELLER IN FLIGHT INCLUDING CONSIDERATIONS
OF THE CHORDWISE BLADE LOADING

By Charles E. Watkins and Barbara J. Durling

Langley Aeronautical Laboratory
Langley Field, Va.



Washington

November 1956

AFMDC
TECHNICAL LIBRARY
TEL 2311



0066769

TECHNICAL NOTE 3809

A METHOD FOR CALCULATION OF FREE-SPACE SOUND PRESSURES

NEAR A PROPELLER IN FLIGHT INCLUDING CONSIDERATIONS

OF THE CHORDWISE BLADE LOADING

By Charles E. Watkins and Barbara J. Durling

SUMMARY

The general expressions of NACA Report 1198 for determining the sound-pressure field for a rotating propeller in uniform subsonic flight are reviewed for the case of a propeller with uniform chordwise forces. Consideration is given to effects of nonuniform chordwise and radial blade loading. Tabulated values of certain definite integrals that are involved in the calculation of a near-field propeller noise regardless of the form of the chordwise forces are presented. These tabulations cover a wide range of operating conditions and are useful for estimating propeller noise when either the concept of an effective radius or radial distributions of forces are considered. In order to illustrate their use, the tabulations are used in conjunction with the concept of an effective radius to make evaluations for some specific propellers. Results of these evaluations are presented and discussed.

INTRODUCTION

In references 1 and 2 the sound-pressure field of an "on-stand" propeller is analyzed by replacing the normal-pressure distributions associated with thrust and torque over the propeller by distributions of pressure doublets acting at the propeller disk. In reference 3 the analyses of references 1 and 2 are extended to the case of an in-flight propeller by considering the pressure doublets that represent the thrust and torque to be subjected to a uniform rectilinear motion.

In references 1 and 3 the equations for the sound pressure are derived in exact form, that is, within the realm of linearized potential theory. For convenience in calculation, however, these equations are ultimately simplified so that they pertain only to the first few harmonics of a propeller of low solidity. These simplifications involve the assumptions that the radial load distribution on a propeller blade can be considered as concentrated at some effective radial position and that the

propeller blade chord is so small that the chordwise load at any radial station can be considered as having the form of an impulse or Dirac delta function. Calculations in references 1 to 3 are based on these assumptions.

The present report begins with the general equations that are derived in reference 3 for the sound field of an in-flight propeller and reviews the specialization of these equations to the case of a uniform or rectangular-type chordwise loading. It is deduced from results for this case that, as long as the chordwise loading remains unchanged throughout the propeller cycle, certain definite integrals involved in the expressions for the sound field are the same regardless of the form of the chordwise loading. In the case of the "far field," or for field points located at distances of several propeller diameters from the propeller, the definite integrals can be evaluated in terms of Bessel functions of the first kind, but, in the case of the "near field" or for field points located within a distance of two or three propeller diameters from the propeller, the integrals must be evaluated by numerical procedures. These numerical evaluations for the near-field case can be made once and for all, however, so as to apply to any chordwise loading that remains unchanged throughout the propeller cycle. A main purpose of this report is therefore to present tabulated values of these definite integrals for a range of parameters that correspond to a large range of operating conditions so that the sound field of a given propeller can be fairly rapidly estimated.

Other purposes of the report are: (a) to consider the effects on the sound field of nonuniform types of chordwise blade loading, (b) to consider a method of evaluating expressions for the sound field when radial distributions of loading are taken into account, and (c) to present and discuss results of some calculations, based on the tabulated integrals, of the sound pressures for some specific propellers. The reduction of definite integrals pertaining to the far-field case to Bessel functions of the first kind and a Fourier series development of some simple shapes that are useful for representing nonuniform chordwise force distributions are presented in the appendixes.

SYMBOLS

B	number of propeller blades
b(r)	width of propeller blades or blade chord
c	velocity of sound
c_n	section normal-force coefficient

D propeller diameter

$F(r, \theta, t)$ chordwise distribution of forces perpendicular to thrust of propeller blade and giving rise to torque

G_1, G_2 functions defined in equations (31) and (32)

$I_\nu, I_\nu, I_\nu', I_\nu''$ functions defined in equations (13), (15), (18), and (19)

J_n Bessel function of first kind with index n

$$K_1 = \frac{2\beta^2 r y}{x^2 + \beta^2 y^2 + \beta^2 r^2}$$

$$K_2 = \frac{\Omega}{\beta^2 c} \sqrt{x^2 + \beta^2 y^2 + \beta^2 r^2}$$

$$k = \omega/c$$

M Mach number, V/c

M_F flight Mach number

M_R rotational Mach number

M_t tip Mach number

m order of harmonic

n propeller rotational speed

p_T pressure due to thrust

p_Q pressure due to torque

p_{rms} root-mean-square pressure

Q torque

R length (radius) of propeller blades

R_e effective (radius) length of propeller blades

R.P. real part of any expression

r radius to blade element

r, θ polar coordinates in yz-plane

$$S = \sqrt{x^2 + \beta^2 y^2 + \beta^2 r^2 - 2\beta^2 r y \cos \theta}$$

T thrust

t time

t' dummy variable

V forward velocity

V_F forward flight velocity

V_t tip velocity

x, y, z, y_1, z_1 Cartesian coordinates

$$\beta = \sqrt{1 - M^2}$$

$\beta_{0.75R}$ blade angle at 0.75 tip radius

μ_1, μ_2 constants

η propeller efficiency

$$\sigma = \frac{Mx + S}{\beta^2}$$

$$\tau = b/r\Omega$$

τ_0 period, $2\pi/B\Omega$

Ω angular velocity

ω frequency of mth harmonic, $mB\Omega$

Subscripts:

j jth element

lt left triangle

r rectangle

rt right triangle

t triangle

$\nu = 1, 2, \text{ and } 3$

ANALYSIS

The sound-pressure equations for chordwise rectangular loading are derived and reduced to expressions involving certain definite integrals denoted by I_ν ($\nu = 1, 2, \text{ and } 3$). It is deduced that the integrals I_ν are common to propeller-noise theory; hence, they are evaluated and tabulated over useful ranges of certain key parameters. This tabulation is discussed briefly and then consideration is given to effects of other types of chordwise loading and to a method of approximating a radial integration involved in the sound-pressure equations.

Sound-Pressure Equations for Chordwise Rectangular

Blade Loading

Although the main purpose of this report is to present tables of certain definite integrals that arise in expressions for the near sound field of a propeller, it is desirable, for the sake of completeness and discussion, to derive the integrals by specializing the general expression for the sound field to some particular form of chordwise loading. For this purpose the general equations derived in reference 3 are specialized to the case of rectangular chordwise loading. More general types of loading are discussed in a subsequent section.

From equations (6) to (12) of reference 3, the equations for the sound pressure p_T associated with a thrust distribution $F_1(t, r, \theta)$ and the sound pressure p_Q associated with a torque distribution $F_2(t, r, \theta)$, F_1 and F_2 being periodic with respect to time, can be written as (see fig. 1 for illustration of coordinate system):

$$p_T = -\frac{1}{4\pi} \int_0^R \int_0^{2\pi} F_1(t, r, \theta) \frac{\partial}{\partial x} \frac{e^{-ikr}}{s} dr d\theta \quad (1)$$

and

$$p_Q = \frac{1}{4\pi} \int_0^R \int_0^{2\pi} F_2(t, r, \theta) \frac{1}{r} \frac{\partial}{\partial \theta} \frac{e^{-ik\sigma}}{S} dr d\theta \quad (2)$$

In these equations R is radius, r is the blade element radius, t is time, θ is a polar angle in the yz -plane, $\beta = \sqrt{1 - M_F^2}$, $S = \sqrt{x^2 + \beta^2 y^2 + \beta^2 r^2 - \beta^2 r y \cos \theta}$, and $\sigma = \frac{Mx + S}{\beta^2}$; $k = \frac{\omega}{c} = \frac{mB\Omega}{c}$ is a frequency parameter involving order of harmonic m , number of blades B , angular velocity Ω , and velocity of sound c . It is to be noted that the expressions for p_T and p_Q (eqs. (1) and (2)) have been made independent of the coordinate z . This is a convenient simplification that follows from rotational symmetry when the loading is assumed to remain unchanged throughout the propeller cycle.

When the periodic functions F_1 and F_2 are known, they can be expressed in the form of Fourier series that enables one to treat each harmonic of the associated noise spectra separately. When, for simplicity, the forces acting on the propeller are assumed to be uniformly distributed at each radial station of the propeller blade, that is, when the chordwise distributions of forces are assumed to be rectangular, the functions $F_1(t, r, \theta)$ and $F_2(t, r, \theta)$ may be expressed, first for $\theta = 0$, as (see ref. 3)

$$\left. \begin{aligned} F_1(t, r, 0) &= \frac{1}{B} \frac{dT}{dr} \frac{r}{b} \frac{d\theta}{dr} dr & (0 < t < \tau) \\ F_1(t, r, 0) &= 0 & (\tau < t < \tau_0) \end{aligned} \right\} \quad (3)$$

$$\left. \begin{aligned} F_2(t, r, 0) &= \frac{1}{B} \frac{1}{r} \frac{dQ}{dr} \frac{r}{b} \frac{d\theta}{dr} dr & (0 < t < \tau) \\ F_2(t, r, 0) &= 0 & (\tau < t < \tau_0) \end{aligned} \right\} \quad (4)$$

where T is thrust, b is blade chord, Q is torque, $\tau = \frac{b}{r\Omega}$ is the time elapsed for a blade chord with angular velocity Ω to pass a given point, and $\tau_0 = \frac{2\pi}{B\Omega}$ is time elapsed for corresponding parts (for example, the leading edges) of two consecutive blades to pass a given point.

The expressions for $F_1(t, r, 0)$ and $F_2(t, r, 0)$ in equations (3) and (4), respectively, may be harmonically analyzed to yield

$$\begin{aligned} F_1(t, r, 0) &= \frac{r}{bB\tau_0} \frac{dT}{dr} d\theta dr \sum_{m=-\infty}^{\infty} \int_0^{\tau} e^{\frac{2m\pi i}{\tau_0}(t-t')} dt' \\ &= \frac{1}{\pi} \sum_{-\infty}^{\infty} \frac{r}{mbB} \left(\sin \frac{mbB}{2r} \right) e^{imB\Omega \left(t - \frac{b}{2\Omega r} \right)} \frac{dT}{dr} dr d\theta \end{aligned} \quad (5)$$

and

$$F_2(t, r, 0) = \frac{1}{\pi} \sum_{-\infty}^{\infty} \frac{r}{mbB} \left(\sin \frac{mbB}{2r} \right) e^{imB\Omega \left(t - \frac{b}{2\Omega r} \right)} \frac{1}{r} \frac{dQ}{dr} dr d\theta \quad (6)$$

In these expression the zeroeth harmonic, $m = 0$, corresponds to the instantaneous average thrust and torque over the blade element which does not give rise to the rotational-type noise under consideration and need not be considered further in the present analysis. For all other harmonics the expressions in equations (5) and (6) may be written as

$$F_1(t, r, 0) = \frac{1}{\pi} R.P. \sum_{m=1}^{\infty} \frac{2r}{mbB} \left(\sin \frac{mbB}{2r} \right) e^{imB\Omega \left(t - \frac{b}{2\Omega r} \right)} \frac{dT}{dr} dr d\theta \quad (7)$$

and

$$F_2(t, r, 0) = \frac{1}{\pi} R.P. \sum_{m=1}^{\infty} \frac{2r}{mbB} \left(\sin \frac{mbB}{2r} \right) e^{imB\Omega \left(t - \frac{b}{2\Omega r} \right)} \frac{1}{r} \frac{dQ}{dr} dr d\theta \quad (8)$$

Although only the real parts of the summations in equations (7) and (8) are necessary in the formulation of the forces, it is convenient to deal with expressions of the forces in complex form throughout the analysis and then, for final results, extract only real parts. Expressions for F_1 and F_2 that pertain to any value of θ may be obtained directly from the expressions in equations (7) and (8) for $\theta = 0$, because the forces on a second blade element that is shifted with respect to the first by an angle θ in the rotational direction are the same as the forces on the first but are retarded by the time θ/Ω . The corresponding Fourier developments are therefore real parts of

$$F_1(t, r, \theta) = \frac{1}{\pi} \sum_{m=1}^{\infty} \frac{2r}{mbB} \left(\sin \frac{mbB}{2r} \right) e^{imB\Omega \left(t - \frac{\theta}{\Omega} - \frac{b}{2\pi r} \right)} \frac{dT}{dr} dr d\theta \quad (9)$$

and

$$F_2(t, r, \theta) = \frac{1}{\pi} \sum_{m=1}^{\infty} \frac{2r}{mbB} \left(\sin \frac{mbB}{2r} \right) e^{imB\Omega \left(t - \frac{\theta}{\Omega} - \frac{b}{2\pi r} \right)} \frac{1}{r} \frac{dQ}{dr} dr d\theta \quad (10)$$

It can be seen from this development that, regardless of the form of the chordwise loading employed, that is, as long as the loading remains unchanged throughout the propeller cycle, the variable θ will always enter into the Fourier development of the forces in the same manner. As will be discussed subsequently, this relationship leads to a fixed set of integrals in the expressions for the sound field.

With the use of equations (9) and (10) for $F_1(t, r, \theta)$ and $F_2(t, r, \theta)$ the equations for the sound pressure associated with thrust and torque (eqs. (1) and (2)) corresponding to rectangular chordwise loading can be written for any harmonic different from zero as

$$p_T = - \frac{e^{i\omega t}}{4\pi^2} \int_0^R \frac{2r}{mbB} \left(\sin \frac{mbB}{2r} \right) \frac{dT}{dr} e^{-\frac{imBb}{2r}} dr \int_0^{2\pi} e^{-imB\theta} \frac{\partial}{\partial x} \frac{e^{-ikx}}{S} d\theta \quad (11a)$$

or

$$p_T = - \frac{e^{i\omega t}}{4\pi^2} \int_0^R \frac{2r}{mbB} \left(\sin \frac{mbB}{2r} \right) \frac{dT}{dr} e^{-\frac{imBb}{2r}} \left[\frac{ikM_F}{\beta^2} \Pi_1(r) + \frac{ikx}{\beta^2} \Pi_2(r) + x \Pi_3(r) \right] dr \quad (11b)$$

and

$$p_Q = \frac{e^{i\omega t}}{4\pi^2} \int_0^R \frac{2r}{mbB} \left(\sin \frac{mbB}{2r} \right) \frac{1}{r} \frac{dQ}{dr} e^{-\frac{imBb}{2r}} dr \int_0^{2\pi} e^{-imB\theta} \frac{1}{r} \frac{\partial}{\partial \theta} \frac{e^{-ik\theta}}{S} d\theta \quad (12a)$$

or

$$p_Q = \frac{imBe^{i\omega t}}{4\pi^2} \int_0^R \frac{2r}{mBb} \left(\sin \frac{mBb}{2r} \right) \frac{1}{r^2} \frac{dr}{dr} e^{-\frac{imBb}{2r}} \Pi_1(r) dr \quad (12b)$$

where

$$\Pi_\nu(r) = \int_0^{2\pi} \frac{e^{-i(mB\theta+k\sigma)}}{s^\nu} d\theta \quad (\nu = 1, 2, \text{ and } 3) \quad (13)$$

In the limit $b = 0$, these expressions for p_T and p_Q are equivalent to those given in equations (21) and (23) of reference 3. This equivalency may be easily verified by use of the limiting value of

$$\lim_{b \rightarrow 0} \left[\frac{2r}{mBb} \left(\sin \frac{mBb}{2r} \right) e^{-\frac{imBb}{2r}} \right] = 1$$

The integrals in equations (11) to (13) must, in general, be evaluated by approximate or numerical procedures. The integrals Π_ν (for $\nu = 1, 2, \text{ and } 3$) in equation (13) occur in expressions for propeller noise regardless of the form of chordwise loading employed, that is, provided the loading remains unchanged throughout the propeller cycle. These integrals therefore play an important role in the analytical determination of propeller noise and are the integrals for which the treatment and evaluations, pertaining to the near field, constitute the main purpose of this report. In the case of the far field the integrals Π_ν can, as was done in references 1 and 3, be reduced to Bessel functions of the first kind. This reduction is, for the sake of completeness, carried out in appendix A in a slightly different and more extended form than was done in references 1 and 3.

The Integrals Π_ν in Terms of Lumped Parameters m_b , K_1 ,
and K_2 and Equivalent Integrals I_ν

The integrals Π_ν are functions of six parameters (x , y , r , M_F , mB , and k). These parameters can be lumped, however, so that the integrals can be conveniently expressed in terms of related integrals that are functions of only three parameters (mB , K_1 , and K_2). This lumping is accomplished as follows:

$$\Pi_\nu = \int_0^{2\pi} \frac{e^{-i(mB\theta+k\sigma)}}{s^\nu} d\theta = e^{-\frac{ikx}{\beta^2}} \int_0^{2\pi} \frac{e^{-imB(\theta + \sqrt{x^2 + \beta^2 y^2 + \beta^2 r^2 - 2\beta^2 ry \cos \theta})}}{(x^2 + \beta^2 y^2 + \beta^2 r^2 - 2\beta^2 ry \cos \theta)^{\nu/2}} d\theta$$

or

$$\Pi_\nu(r) = \left(\frac{\Omega}{\beta^2 c}\right)^\nu e^{-\frac{ikM_F x}{\beta^2}} I_\nu(r) = \left(\frac{M_R}{\beta^2 R K_2}\right)^\nu e^{-\frac{ikM_F x}{\beta^2}} I_\nu(r) \quad (14)$$

where

$$I_\nu(r) = \int_0^{2\pi} \frac{e^{-imB(\theta + K_2 \sqrt{1 - K_1 \cos \theta})}}{(\sqrt{1 - K_1 \cos \theta})^\nu} d\theta = I_\nu' - iI_\nu'' \quad (15)$$

$$K_1 = \frac{2\beta^2 r y}{x^2 + \beta^2 y^2 + \beta^2 r^2} = \frac{2\beta^2 \frac{r}{R} \frac{y}{R}}{\left(\frac{x}{R}\right)^2 + \beta^2 \left(\frac{y}{R}\right)^2 + \beta^2 \left(\frac{r}{R}\right)^2} \quad (16)$$

$$\begin{aligned} K_2 &= \frac{\Omega}{\beta^2 c} \sqrt{x^2 + \beta^2 y^2 + \beta^2 r^2} \\ &= \frac{\Omega R}{\beta^2 c} \sqrt{\left(\frac{x}{R}\right)^2 + \beta^2 \left(\frac{y}{R}\right)^2 + \beta^2 \left(\frac{r}{R}\right)^2} \\ &= \frac{M_R}{\beta^2} \sqrt{\left(\frac{x}{R}\right)^2 + \beta^2 \left(\frac{y}{R}\right)^2 + \beta^2 \left(\frac{r}{R}\right)^2} \end{aligned} \quad (17)$$

and M_R denotes the Mach number associated with rotational velocity.
The integrals I_ν' and I_ν'' may be expressed as

$$I_\nu' = \int_0^{2\pi} \frac{\cos mB(\theta + K_2 \sqrt{1 - K_1 \cos \theta})}{(\sqrt{1 - K_1 \cos \theta})^\nu} d\theta \quad (18a)$$

or

$$I_\nu' = 2e^{-imB\pi} \int_0^\pi \frac{\cos mB\theta \cos mBK_2 \sqrt{1 + K_1 \cos \theta}}{(\sqrt{1 + K_1 \cos \theta})^\nu} d\theta \quad (18b)$$

and

$$I_v'' = \int_0^{2\pi} \frac{\sin mB(\theta + K_2 \sqrt{1 - K_1 \cos \theta})}{(\sqrt{1 - K_1 \cos \theta})^v} d\theta \quad (19a)$$

or

$$I_v'' = 2e^{-imB\pi} \int_0^\pi \frac{\cos mB\theta \sin mBK_2 \sqrt{1 + K_1 \cos \theta}}{(\sqrt{1 + K_1 \cos \theta})^v} d\theta \quad (19b)$$

Expressions for the pressures p_T and p_Q in terms of the integrals I_v may be written as

$$\begin{aligned} p_T = & - \frac{M_R^2 e^{imB\left(\Omega t - \frac{M_F M_R}{\beta^2} \frac{x}{R}\right)}}{4\pi^2 \beta^2 R^2 K_2} \int_0^R \frac{2r}{mBb} \left(\sin \frac{mBb}{2r} \right) \frac{dT}{dr} e^{-\frac{imBb}{2r}} \left[\left(\frac{mBM_F}{R} I_1'' + \right. \right. \\ & \left. \left. \frac{x}{R} \frac{mBM_R}{\beta^2 K_2} I_2'' + \frac{x}{R} \frac{M_R}{\beta^2 K_2^2} I_3' \right) + i \left(\frac{mBM_F}{R} I_1' + \right. \right. \\ & \left. \left. \frac{x}{R} \frac{mbM_R}{\beta^2 K_2} I_2' - \frac{x}{R} \frac{M_R}{\beta^2 K_2^2} I_3'' \right) \right] dr \end{aligned} \quad (20)$$

and

$$p_Q = \frac{mBM_R e^{imB\left(\Omega t - \frac{M_F M_R}{\beta^2} \frac{x}{R}\right)}}{4\pi^2 \beta^2 R K_2} \int_0^R \frac{2r}{mBb} \left(\sin \frac{mBb}{2r} \right) \frac{1}{r^2} \frac{dQ}{dr} e^{-\frac{imBb}{2r}} (I_1'' + iI_1') dr \quad (21)$$

Tables of I_v Corresponding to the Near Field

Since the integrals I_v are expressed in terms of lumped parameters K_1 (eq. (16)) and K_2 (eq. (17)), it is necessary to determine the range of values of these parameters that pertain to the near field and to the far field. Regardless of the values that x , y , r , and β

may have, numerical values of K_1 will always fall in the range

$$0 \leq K_1 \leq 1 \quad (22)$$

but numerical values of K_2 fall in the semi-infinite range

$$0 \leq K_2 \leq \infty \quad (23)$$

Inasmuch as the present development is inherently restricted to propeller tip speeds V_t that correspond to propeller-tip Mach numbers M_t less than about unity, the factor $\frac{M_R}{\beta^2} = \frac{M_R}{1 - M_F^2}$ of K_2 does not become large even when M approaches 1. This condition exists because

$$M_t = \sqrt{\left(\frac{V_F}{c}\right)^2 + \left(\frac{\Omega R}{c}\right)^2} = \sqrt{M_F^2 + M_R^2} \quad (24)$$

thus, when $M_F \approx 1$, $M_R \approx 0$ for $M_t \approx 1$. It therefore follows that large numerical values of K_2 are associated only with large values of $\sqrt{x^2 + \beta^2 y^2}$ and these large values imply large distances from the propeller disk. Furthermore, large distances from the propeller disk imply small numerical values of K_1 ($K_1 \ll 1$). Hence, small values of K_1 and large values of K_2 ($K_2 \gg 1$) apply to the far field and large values of K_1 and small values of K_2 pertain to the near field. The specific ranges of values of K_1 and K_2 considered in the present report for the near field are $0.4 \leq K_1 \leq 0.985$ and $0.75 \leq K_2 \leq 6.0$, respectively. These ranges correspond to distances less than about 2.5 propeller diameters from the propeller tip. Tables of values of the integrals I_ν that cover these ranges of K_1 and K_2 for a number of values of the parameter mB are presented in tables I to VII. Evaluations are presented for values of mB of 2, 3, 4, 6, 8, 9, and 12; values of K_1 of 0.4, 0.5, 0.6, 0.7, 0.75, 0.8, 0.85, 0.9, 0.925, 0.95, and 0.985; and values of K_2 at intervals of 0.25 in the range $0.75 \leq K_2 \leq 6.0$.

The evaluations were made with the use of a card-programmed electronic calculator and are presented, as calculated, to eight significant figures. They can be considered accurate throughout, however, to no more than four significant figures. In order to maintain this accuracy throughout the calculations, it was necessary to decrease the θ -increments at which the

integrands were evaluated in making the numerical integrations as the parameter mB was increased. The specific increments employed are for values of mB of 2, 3, and 4, $\Delta\theta = 6^\circ$; for a value of mB of 6, $\Delta\theta = 4^\circ$; and for values of mB of 8, 9, and 12, $\Delta\theta = 3^\circ$. With regard to interpolation in the tables, the increments in K_1 and K_2 are not small enough to yield good results by linear interpolation. Reasonably good interpolated results can be obtained, however, by graphical procedures or by a nonlinear scheme such as Aitken's method.

Consideration of Effects of Other Types of Chordwise Loading

It is recalled that the equations for the sound field of propellers derived in foregoing sections of this report are based on the assumption of a uniform chordwise loading. With real propellers, however, the actual form of the chordwise loading, which is, of course, not uniform, may be very significant with regard to the generation of rotational noise. For example, a propeller may be loaded, as in "turn ups", so as to produce no net thrust, yet it may produce considerable noise, mainly of a higher harmonic content. The fact is that negative forces produce noise as well as positive forces and it is only when the separate forces are in one direction that the assumption of uniform loading over the chord should be expected to yield realistic values for the calculated noise. Some examples that bear out this statement and demonstrate the significance of nonuniform chordwise loading are presented in the following paragraphs.

Examples based on square-wave type chordwise loading.— Consider first a propeller to have a constant loading F_0 on the front half-chord and constant loading $-F_0$ on the rear half-chord of a section of each blade at some radial station r . That is, let a force acting on each blade be defined by

$$\left. \begin{aligned} f(t, r, \theta) &= \frac{r}{bB} F_0 & (0 < t < \frac{\tau}{2}) \\ f(t, r, \theta) &= -\frac{r}{bB} F_0 & (\frac{\tau}{2} < t < \tau) \\ f(t, r, \theta) &= 0 & (\tau < t < \tau_0) \\ f(t+\tau_0, r, \theta) &= f(t, r, \theta) \end{aligned} \right\} \quad (25)$$

This function corresponds to a zero net force and may be written as a Fourier series, with the zeroeth harmonic neglected, as

$$f(t, r, \theta) = R.P. \frac{4F_0}{\pi} \sum_{m=1}^{\infty} \frac{ir}{mBb} \left(\sin^2 \frac{mB}{4} \frac{b}{r} \right) e^{imB \left(\Omega t - \theta - \frac{b}{2r} \right)} \quad (26)$$

Next, for the sake of comparison, consider the full-wave rectification of $f(t, r, \theta)$. That is,

$$\left. \begin{aligned} |f(t, r, \theta)| &= \frac{r}{Bb} F_0 & (0 < t < \tau) \\ |f(t, r, \theta)| &= 0 & (\tau < t < \tau_0) \\ |f(t + \tau_0, r, \theta)| &= |f(t, r, \theta)| \end{aligned} \right\} \quad (27)$$

The Fourier expansion of this function is found to be, the zeroeth harmonic being neglected

$$|f(t, r, \theta)| = R.P. \frac{2F_0}{\pi} \sum_{m=1}^{\infty} \frac{r}{mBb} \left(\sin \frac{mBb}{2r} \right) e^{imB \left(\Omega t - \theta - \frac{b}{2r} \right)} \quad (28)$$

It may be noted that there is a phase difference of 90° , indicated by the pure imaginary term in equation (26), between the harmonics of $f(t, r, \theta)$ and $|f(t, r, \theta)|$. The main thing of interest in the present discussion, however, is the relative values of the amplitude functions

$\frac{4r}{mBb} \sin^2 \frac{mBb}{4r}$ of $f(t, r, \theta)$ and $\frac{2r}{mBb} \sin \frac{mBb}{2r}$ of $|f(t, r, \theta)|$. These functions are shown plotted as a function of $\frac{mBb}{2r}$ in figure 2. Exam-

ination of this figure shows that, for a range of values of $\frac{mBb}{2r} > \frac{\pi}{2}$, the amplitude function for $f(t, r, \theta)$ is greater than that for $|f(t, r, \theta)|$ even though the function $f(t, r, \theta)$ corresponds to no net force.

Examples based on measured distributions of normal force. - Under actual operating conditions the chordwise distribution of force is usually such that it can be closely approximated with the use of a few simple shapes such as rectangles and triangles. Furthermore, the Fourier development for such shapes can be made once and for all in such a way that, when a chordwise force distribution is known, its Fourier development can be obtained by simple superposition. In order to illustrate this point and to demonstrate further the significance of negative loading with regard to sound pressures, two cases of measured distribution of normal-force coefficients chosen from reference 4 are plotted in figure 3 for the operating conditions shown. Each of the two chosen distributions is for a blade section at $r = 0.78R$; however, one distribution (fig. 3(a)) corresponds to a small net loading with negative forces acting over part of the chord, and the other distribution (fig. 3(b)) corresponds to a large net loading with no negative forces. The area under each curve is divided into rectangles and triangles by the dashed lines shown in figure 3. (The right triangle facing to the right is herein designated right triangle, and the right triangle facing to the left is herein designated left triangle. Their elements are designated right triangular and left triangular, respectively.) The Fourier developments of arbitrarily placed rectangular- and right and left triangular-shaped elements of loading are given in appendix B and have been employed to obtain the Fourier expansions of the distributions in figure 3. The amplitudes so obtained are plotted as a function of mB in figure 4 and compared with amplitude functions for uniform chordwise loading that yield the same net values as do the distributions in figure 3 and with amplitude functions associated with Dirac delta-type loadings. The results in figure 4(a) are for the case of low net loading and these results show that taking into account the negative forces as well as the positive forces can lead to considerably higher amplitude of sound in the higher harmonics. The results in figure 4(b) for the case of no negative forces show that about the same level of noise is obtained from the uniform distribution of forces as from the detailed distribution of forces. The amplitude functions for the Dirac delta-type loadings agree, as would be expected, with those for rectangular-type loading for lower values of mB .

The Integrations in the Radial Direction

A brief consideration is now given to a method of approximating the integrations with respect to r indicated in equations (11) and (12). These integrations can be accomplished by a generalization of the concept of effective radius discussed in references 1 to 3. As discussed in these references, the concept of effective radius is based on the consideration that all the sound-producing forces acting on the propeller can be assumed to be concentrated on an annular ring that roughly coincides with the circumference along which the resultant force acts.

In the present case the assumption of an effective radius $r = R_e$ gives, from equations (20) and (21),

$$\begin{aligned}
 p_T &= - \frac{M_R^2 e^{imB\left(\Omega t - \frac{M_F M_R}{\beta^2} \frac{x}{R}\right)}}{4\pi^2 \beta^4 R^2 K_2(R_e)} G_1(R_e) \int_0^R \frac{dT}{dr} dr \\
 &= - \frac{M_R^2 e^{imB\left(\Omega t - \frac{M_F M_R}{\beta^2} \frac{x}{R}\right)}}{4\pi^2 \beta^4 R^2 K_2(R_e)} TG_1(R_e)
 \end{aligned} \tag{29}$$

and

$$\begin{aligned}
 p_Q &= \frac{mBM_R e^{imB\left(\Omega t - \frac{M_F M_R}{\beta^2} \frac{x}{R}\right)}}{4\pi^2 \beta^2 R K_2(R_e)} G_2(R_e) \int_0^R \frac{dQ}{dr} dr \\
 &= \frac{mBM_R e^{imB\left(\Omega t - \frac{M_F M_R}{\beta^2} \frac{x}{R}\right)}}{4\pi^2 \beta^2 R K_2(R_e)} QG_2(R_e)
 \end{aligned} \tag{30}$$

where

$$\begin{aligned}
 G_1(R_e) &= F_m\left(\frac{mBb}{R_e}\right) \left(\left\{ mBM_F I_1''(R_e) + \frac{x}{R_e} \frac{mBM_R}{\beta^2 K_2(R_e)} I_2''(R_e) + \frac{x}{R} \frac{M_R}{\beta^2 [K_2(R_e)]^2} I_3'(R_e) \right\} + \right. \\
 &\quad \left. i \left\{ mBM_F I_1'(R_e) + \frac{x}{R} \frac{mBM_R}{\beta^2 K_2(R_e)} I_2'(R_e) - \frac{x}{R} \frac{M_R}{\beta^2 [K_2(R_e)]^2} I_3''(R_e) \right\} \right)
 \end{aligned} \tag{31}$$

$$G_2(R_e) = F_m\left(\frac{mBb}{R_e}\right) \frac{1}{R_e^2} \left[I_1''(R_e) + iI_1'(R_e) \right] \quad (32)$$

and $F_m\left(\frac{mBb}{R_e}\right)$ is an amplitude function that depends on the form of the chordwise blade loading. For uniform or rectangular-type chordwise loading (see eqs. (20) and (21)),

$$F_m = \frac{2R_e}{mBb} \left(\sin \frac{mBb}{2R_e} \right) e^{-\frac{imBb}{2R_e}}$$

In many cases, especially when the point at which the sound pressure is to be calculated is outside and not too near the cylinder formed by the propeller disk and its wake, the total sound pressure is evidently not sensitive to the details of the radial distribution of forces; thus, the assumption of an effective radius serves as a means of approximating the total sound pressure. See, for example, comparisons of calculated and measured results in references 1 and 2. For cases where details of the radial loading are important, as would be true, for example, at near-field points inside the cylinder formed by the propeller disk and its wake, the effective-radius concept can be generalized as follows:

Suppose the distributions of thrust and torque are graphically represented as indicated in the sketch in figure 5. Divide the areas under the curve into n parts by dividing the blade length R into n parts. The parts into which R is divided need not be equal but they should be fairly small to insure a reasonably accurate approximation to the integrations. Let $R_{e,j}$ denote the abscissa of the center of area of the j th element of area under the curve. Approximate expressions for p_T and p_Q (eqs. (20) and (21)) may then be written as

$$p_T = - \frac{\frac{M_R^2}{4\pi^2\beta^2 R^2} e^{imB\left(\Omega t - \frac{M_R M_F}{\beta^2} \frac{x}{R}\right)}}{\sum_{j=1}^n \frac{G_1(R_{e,j})}{K_2(R_{e,j})} \Delta T_j} \quad (33)$$

and

$$p_Q = \frac{\frac{mBM_R}{4\pi^2\beta^2 R} e^{imB\left(\Omega t - \frac{M_R M_F}{\beta^2} \frac{x}{R}\right)}}{\sum_{j=1}^n \frac{G_2(R_{e,j})}{K_2(R_{e,j})} \Delta Q_j} \quad (34)$$

where $G_1(R_e, j)$ and $G_2(R_e, j)$ are defined in equations (31) and (32), respectively, and

$$\Delta T_j = \int_{r_j}^{r_{j+1}} \frac{dT}{dr} dr \quad (35)$$

and

$$\Delta Q_j = \int_{r_j}^{r_{j+1}} \frac{dQ}{dr} dr \quad (36)$$

are the j th elements of area under the radial distributions of thrust and torque curves.

Root-Mean-Square Value of Pressure

Before some specific examples are discussed, it is appropriate to point out that, in applications of propeller noise theory, one is generally interested in the magnitude of the root mean square of the total pressure P_{rms} for each harmonic of noise. In order to obtain this quantity, it is convenient to treat the propeller forces as complex quantities. As may be noted in equations (20) and (21) or equations (33) and (34) the pressures p_T and p_Q are of forms

$$p_T = (\cos \omega t + i \sin \omega t)(A_1 + iA_2) \quad (37)$$

and

$$p_Q = (\cos \omega t + i \sin \omega t)(B_1 + iB_2) \quad (38)$$

The form of an expression for the total sound pressure p associated with thrust and torque is obtained by adding these expressions and retaining only the real parts of the sum. That is,

$$p = R.P.(p_T + p_Q) = (A_1 + B_1)\cos \omega t - (A_2 + B_2)\sin \omega t \quad (39)$$

The root-mean-square value of this expression is

$$\begin{aligned}
 p_{rms} &= \left\{ \frac{\omega}{2\pi} \int_0^{2\pi/\omega} [(A_1 + B_1) \cos \omega t - (A_2 + B_2) \sin \omega t]^2 dt \right\}^{1/2} \\
 &= \frac{1}{\sqrt{2}} \sqrt{(A_1 + B_1)^2 + (A_2 + B_2)^2} = \frac{1}{\sqrt{2}} |p_T + p_Q| \quad (40)
 \end{aligned}$$

Thus p_{rms} is obtained by simply multiplying the absolute value of the complex sum $p_T + p_Q$ by $\frac{1}{\sqrt{2}}$.

SOME APPLICATIONS TO SPECIFIC PROPELLERS

The propellers chosen for the applications of the tables are three- and four-blade 16-foot-diameter propellers with solidity factors ranging from 0.12 to 0.16. The efficiency, total thrust, and total torque for such propellers have been determined from charts of references 5 and 6 and are summarized in figure 6. The total thrust for three different altitudes and the efficiency are presented as functions of flight Mach number M_F in figures 6(a) and 6(b), respectively. The total torque is presented as a function of rotational Mach number M_R in figure 6(c).

The present examples are based on the assumption of uniform chordwise loading and, except for one case, on the concept of an effective radius (eqs. (29) and (30)) with $R_e = 0.8R$. When the calculated results were obtained, the necessary interpolations in the tables of I_V were performed by graphical procedures.

The first results are presented in figure 7 and are intended to give some indication as to the differences that might be expected between calculations based on the concept of an effective radius and calculations based on radial distributions of forces. Shown in the figure are values of the root-mean-square pressure, associated with the first harmonic of a four-blade 16-foot-diameter propeller, calculated with the use of equations (33) and (34) (by using five steps), for radial distributions of forces shown in the upper plot and calculated with the use of equations (29) and (30) for the forces assumed to be concentrated on an annulus of radius 0.8R. Calculations by each procedure were made for operating conditions indicated in figure 7 at various values of x in the range $-0.3D \leq x \leq 0.3D$ along a line $y = 0.7D$ (11.2 feet); that is, along a line two-fifths of the propeller radius from the tip and extending a distance three-fifths of the radius behind to three-fifths of the radius ahead of the plane of rotation. For the conditions considered, the pressure or sound levels based on distributed forces are below those

based on effective radius or concentrated forces at each point considered. The significant point is that the shapes of the two curves, considered as functions of x/D , are about the same; this fact indicates that calculations based on an effective radius can at least be used for studying trends.

In figure 8 calculated values of the root-mean-square pressure associated with the first harmonic of a four-blade 16-foot-diameter propeller are plotted as functions of x/D for two altitude conditions, three values of rotational Mach number M_R , and a fixed value (0.6) of flight Mach number M_F .

As can be noted in figure 8 for the set of conditions under consideration, the peaks or highest amplitudes of pressure occur behind the plane of rotation at values of x/D in the range from -0.05 to -0.125. A somewhat surprising feature of the results is the rather sharp rearward trend of the position of peak amplitude as M_R is increased. As noted in reference 3, the trend of position of peak amplitude of pressure with increasing M_F is from some rearward position toward the plane of rotation or just the opposite of that indicated in figure 7 for increasing M_R . The results also indicate a rather sharp attenuation of sound-pressure level with altitude and with distance away from the location of peak amplitude. The apparent attenuation with altitude, however, can be directly associated with the decrease in thrust and torque (see fig. 6) required for the higher altitude.

In figure 9 the calculated root-mean-square pressures associated with the first harmonic of a four-blade, 16-foot-diameter propeller for a point $x = -0.15D$, $y = 11.2$ feet (or $0.7D$) are shown plotted as a function of flight Mach number for three altitude conditions and a fixed rotational Mach number ($M_R = 0.8$). These results show, as do the examples in reference 3, that, for a fixed altitude, the amplitudes of sound pressure decrease substantially with flight Mach number for Mach numbers up to about 0.4 or 0.5 and then increase rapidly with flight Mach number.

Figure 10 shows the effect of flight Mach number on the calculated root-mean-square pressures for various values of the parameter mB for two altitude conditions. The calculations are for a point $x = 0$, $y = 11.2$ feet (or $0.7D$) and for a fixed value of the rotational Mach number ($M_R = 0.7$). A change in the parameter mB may correspond to either a change in number of propeller blades B or a change in harmonic m . For example, the curves in figure 10 for $mB = 8$ may be interpreted as the calculated sound pressure corresponding to either the first harmonic of an 8-blade propeller, the second harmonic of a 4-blade propeller, or the fourth harmonic of a 2-blade propeller.

All the curves in figure 10 show the falling-off or diminishing characteristic as the Mach number M_F is increased from zero up to 0.2 or 0.3 and then the rapid increase with Mach number when M_F exceeds about 0.4 or 0.5. The total amount that the calculated pressures decrease from the $M_F = 0$ condition is about the same percentage (about 20) in each case. It may be implied therefore that, in the neighborhood of take-off conditions, the Mach number effect is about the same, percentagewise, regardless of the value of mB . The increase with Mach number, after a Mach number of 0.4 or 0.5 has been attained, however, depends strongly on the value of mB and becomes very large as mB increases beyond 6 or 8. For these large values of mB the present simplified theory, especially with the assumption of an effective radius, could only serve to indicate the trends roughly. In order to yield realistic magnitudes, it is likely that the details of the radial loading and, perhaps, details of the chordwise loadings would have to be taken into account.

The effect of distance from the propeller on the sound level along a line of constant y is implied in figures 7 and 8. Figure 11 shows the corresponding effect along a line of constant x ($x = -0.15D$). The results shown are the calculated root-mean-square pressures corresponding to the first harmonic of a four-blade 16-foot-diameter propeller for $M_F = 0$ and $M_R = 0.7$ at sea level plotted as a function of d/D where d is the distance from the propeller tip. Figure 11 shows that, for the conditions considered, the amplitude of pressure drops off very rapidly as the distance from the propeller tip is increased. This type of dropoff is typical of that expected for other values of the parameters M_F , M_R , and mB .

CONCLUDING REMARKS

A main purpose of this report is to present tabulated values of certain definite integrals that are involved in the calculation of near-field propeller noise. These tabulations cover a wide range of operating conditions and are useful for estimating lower harmonic, near-field propeller noise when either the concept of an effective radius or radial distributions of forces are considered.

Consideration is given to the general forms of chordwise and radial load distributions and it is shown that propellers operating even with zero net forces can give rise to considerable noise, especially in the

higher harmonics. Results of applications of noise theory to some specific 16-foot-diameter propellers are presented and discussed.

Langley Aeronautical Laboratory,
National Advisory Committee for Aeronautics,
Langley Field, Va., June 26, 1956.

APPENDIX A

EVALUATION OF THE INTEGRALS I_ν FOR THE FAR FIELD

As pointed out in the text, the integrals I_ν corresponding to the far field or small values of the parameter K_1 ($K_1 \ll 1$) can be expressed in terms of Bessel functions of the first kind. The purpose of this appendix is to reduce the integrals to such expressions.

For this purpose it is convenient to consider the integral expression for I_ν given in equation (15); that is,

$$I_\nu(r) = \int_0^{2\pi} \frac{e^{-imB(\theta + K_2 \sqrt{1 - K_1 \cos \theta})}}{(\sqrt{1 - K_1 \cos \theta})^\nu} d\theta = I_\nu' - iI_\nu''$$

The value of the radical $\sqrt{1 - K_1 \cos \theta}$ appearing in the exponential term and in the denominator of the integrand of this expression is, for $K_1 \ll 1$, closely approximated by

$$\sqrt{1 - K_1 \cos \theta} \approx 1 - \frac{K_1}{2} \cos \theta \quad (A1)$$

Correspondingly, the integral I_ν is closely approximated by

$$I_\nu \approx \int_0^{2\pi} \frac{e^{-imB\left(\theta + K_2 - \frac{K_1 K_2}{2} \cos \theta\right)}}{\left(1 - \frac{K_1}{2} \cos \theta\right)^\nu} d\theta$$

or

$$I_\nu \approx e^{-imBK_2} \int_0^{2\pi} e^{-imB\left(\theta - \frac{K_1 K_2}{2} \cos \theta\right)} \left(1 + \frac{vK_1}{2} \cos \theta\right) d\theta \quad (A2)$$

From the known integral representation of Bessel functions,

$$\int_0^{2\pi} e^{-i(n\theta - \lambda \cos \theta)} d\theta = 2\pi i^n J_n(\lambda) \quad (A3)$$

and

$$\begin{aligned} \cos \theta e^{-i(n\theta - \lambda \cos \theta)} d\theta &= -i \frac{\partial}{\partial \lambda} \int_0^{2\pi} e^{-i(n\theta - \lambda \cos \theta)} d\theta \\ &= -\pi i^{n+1} [J_{n-1}(\lambda) - J_{n+1}(\lambda)] \end{aligned} \quad (A4)$$

The expression for I_V given in equation (A2) may be written as

$$\begin{aligned} I_V &\approx \pi i^{mB} e^{-imBK_2} \left\{ 2J_{mB} \left(\frac{mBK_1 K_2}{2} \right) - \right. \\ &\quad \left. \frac{i\nu K_1}{2} \left[J_{mB-1} \left(\frac{mBK_1 K_2}{2} \right) - J_{mB+1} \left(\frac{mBK_1 K_2}{2} \right) \right] \right\} \end{aligned} \quad (A5)$$

or, by substituting the relations for K_1 and K_2 ,

$$\begin{aligned} I_V &\approx \pi i^{mB} e^{-\frac{ik}{\beta^2} \sqrt{x^2 + \beta^2 y^2 + \beta^2 r^2}} \left\{ 2J_{mB} \left(\frac{kry}{\sqrt{x^2 + \beta^2 y^2 + \beta^2 r^2}} \right) - \right. \\ &\quad \left. i \frac{\nu \beta^2 ry}{x^2 + \beta^2 y^2 + \beta^2 r^2} \left[J_{mB-1} \left(\frac{kry}{\sqrt{x^2 + \beta^2 y^2 + \beta^2 r^2}} \right) - J_{mB+1} \left(\frac{kry}{\sqrt{x^2 + \beta^2 y^2 + \beta^2 r^2}} \right) \right] \right\} \end{aligned} \quad (A6)$$

or, since $\beta r \ll \sqrt{x^2 + \beta^2 y^2}$ for large distances from the propeller disk,

$$\begin{aligned}
 I_v &\approx \pi i^{mB} e^{-\frac{ik}{\beta^2} \sqrt{x^2 + \beta^2 y^2}} \left\{ 2J_{mB} \left(\frac{kry}{\sqrt{x^2 + \beta^2 y^2}} \right) - \right. \\
 &\quad \left. \frac{i\nu\beta^2 ry}{x^2 + \beta^2 y^2} \left[J_{mB-1} \left(\frac{kry}{\sqrt{x^2 + \beta^2 y^2}} \right) - J_{mB+1} \left(\frac{kry}{\sqrt{x^2 + \beta^2 y^2}} \right) \right] \right\} \\
 &= \pi i^{mB} \left(\left(2 \cos \frac{k}{\beta^2} \sqrt{x^2 + \beta^2 y^2} \right) J_{mB} \left(\frac{kry}{\sqrt{x^2 + \beta^2 y^2}} \right) - \right. \\
 &\quad \left. \frac{\nu\beta^2 ry}{x^2 + \beta^2 y^2} \left(\sin \frac{k}{\beta^2} \sqrt{x^2 + \beta^2 y^2} \right) \left[J_{mB-1} \left(\frac{kry}{\sqrt{x^2 + \beta^2 y^2}} \right) - J_{mB+1} \left(\frac{kry}{\sqrt{x^2 + \beta^2 y^2}} \right) \right] \right) - \\
 &\quad i \left\{ \left(2 \sin \frac{k}{\beta^2} \sqrt{x^2 + \beta^2 y^2} \right) J_{mB} \left(\frac{kry}{\sqrt{x^2 + \beta^2 y^2}} \right) + \right. \\
 &\quad \left. \left. \frac{\nu\beta^2 ry}{x^2 + \beta^2 y^2} \left(\cos \frac{k}{\beta^2} \sqrt{x^2 + \beta^2 y^2} \right) \left[J_{mB-1} \left(\frac{kry}{\sqrt{x^2 + \beta^2 y^2}} \right) - J_{mB+1} \left(\frac{kry}{\sqrt{x^2 + \beta^2 y^2}} \right) \right] \right\} \right) \\
 \end{aligned} \tag{A7}$$

Thus, for mB even,

$$\begin{aligned}
 I_v' &= \pi (-1)^{mB/2} \left\{ \left(2 \cos \frac{k}{\beta^2} \sqrt{x^2 + \beta^2 y^2} \right) J_{mB} \left(\frac{kry}{\sqrt{x^2 + \beta^2 y^2}} \right) - \right. \\
 &\quad \left. \frac{\nu\beta^2 ry}{x^2 + \beta^2 y^2} \left(\sin \frac{k}{\beta^2} \sqrt{x^2 + \beta^2 y^2} \right) \left[J_{mB-1} \left(\frac{kry}{\sqrt{x^2 + \beta^2 y^2}} \right) - J_{mB+1} \left(\frac{kry}{\sqrt{x^2 + \beta^2 y^2}} \right) \right] \right\} \\
 \end{aligned} \tag{A8}$$

and

$$\begin{aligned}
 I_v'' &= \pi (-1)^{mB/2} \left\{ \left(2 \sin \frac{k}{\beta^2} \sqrt{x^2 + \beta^2 y^2} \right) J_{mB} \left(\frac{kry}{\sqrt{x^2 + \beta^2 y^2}} \right) + \right. \\
 &\quad \left. \frac{\nu\beta^2 ry}{x^2 + \beta^2 y^2} \left(\cos \frac{k}{\beta^2} \sqrt{x^2 + \beta^2 y^2} \right) \left[J_{mB-1} \left(\frac{kry}{\sqrt{x^2 + \beta^2 y^2}} \right) - J_{mB+1} \left(\frac{kry}{\sqrt{x^2 + \beta^2 y^2}} \right) \right] \right\} \\
 \end{aligned} \tag{A9}$$

For mB odd,

$$I_v' = \pi(-1)^{\frac{mB-1}{2}} \left\{ \left(2 \sin \frac{k}{\beta^2} \sqrt{x^2 + \beta^2 y^2} \right) J_{mB} \left(\frac{kry}{\sqrt{x^2 + \beta^2 y^2}} \right) + \right.$$

$$\left. \frac{\nu \beta^2 ry}{x^2 + \beta^2 y^2} \left(\cos \frac{k}{\beta^2} \sqrt{x^2 + \beta^2 y^2} \right) \left[J_{mB-1} \left(\frac{kry}{\sqrt{x^2 + \beta^2 y^2}} \right) - J_{mB+1} \left(\frac{kry}{\sqrt{x^2 + \beta^2 y^2}} \right) \right] \right\} \quad (A10)$$

and

$$I_v'' = \pi(-1)^{\frac{mB+1}{2}} \left\{ \left(2 \cos \frac{k}{\beta^2} \sqrt{x^2 + \beta^2 y^2} \right) J_{mB} \left(\frac{kry}{\sqrt{x^2 + \beta^2 y^2}} \right) - \right.$$

$$\left. \frac{\nu \beta^2 ry}{x^2 + \beta^2 y^2} \left(\sin \frac{k}{\beta^2} \sqrt{x^2 + \beta^2 y^2} \right) \left[J_{mB-1} \left(\frac{kry}{\sqrt{x^2 + \beta^2 y^2}} \right) - J_{mB+1} \left(\frac{kry}{\sqrt{x^2 + \beta^2 y^2}} \right) \right] \right\} \quad (A11)$$

These approximations of I_v for the far field go a step beyond that given in reference 3 in that the terms herein involving ν as a factor were not considered in reference 3. It is not deemed necessary to tabulate I_v for the far-field case since tabulations of the Bessel functions J_n are so abundant in the literature.

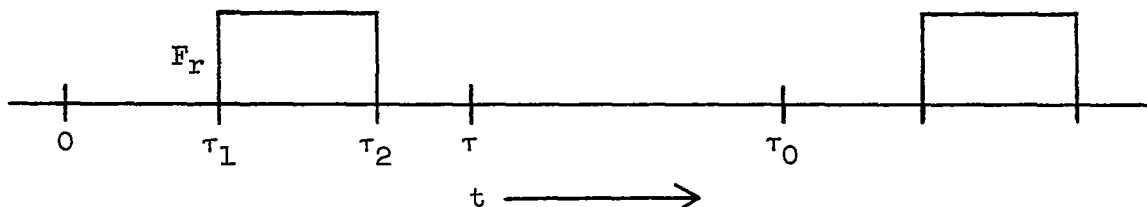
APPENDIX B

THE FOURIER DEVELOPMENT OF SOME SIMPLE SHAPES USEFUL FOR
 REPRESENTING CHORDWISE FORCE DISTRIBUTIONS
 FOR PROPELLER BLADES

It is assumed that any chordwise distribution of force acting on a propeller-blade section can be satisfactorily represented by superimposing rectangular- and triangular-shaped elements of force as indicated in figure 3. This, at least, is a convenient assumption because such elements can be expanded into Fourier series in such a way as to make the Fourier development of the force distribution obtainable by simply adding the Fourier series representations of the different components into which the force distribution is divided.

Rectangular Element of Loading

Consider first a rectangular element of periodic force $f_r(t, r, \theta)$ that is located on some element of chord in a force-time system.



If the origin of coordinates is chosen to be the leading edge of the blade section, f_r may be expressed as follows:

$$\left. \begin{aligned} f_r(t, r, \theta) &= 0 & 0 < t < \tau_1 \\ f_r(t, r, \theta) &= F_r d\theta dr & \tau_1 < t < \tau_2 \\ f_r(t, r, \theta) &= 0 & \tau_2 < t < \tau_0 \\ f_r(t+\tau_0, r, \theta) &= f_r(t, r, \theta) \end{aligned} \right\} \quad (B1)$$

where

$$\tau_1 = \mu_1 \tau = \mu_1 \frac{b}{r\Omega}$$

$$\tau_2 = \mu_2 \tau = \mu_2 \frac{b}{r\Omega}$$

The terms μ_1 and μ_2 are constants such that $0 \leq \mu_1 \leq 1$ and $0 \leq \mu_2 \leq 1$. Equations (B1) may be expressed as a Fourier series, the term corresponding to the zeroeth harmonic being neglected, as

$$\begin{aligned} f_r(t, r, \theta) &= \frac{2F_r d\theta dr}{\tau_0} \sum_{l=1}^{\infty} \left[\cos \frac{2m\pi}{\tau_0} \left(t - \frac{\theta}{\Omega} \right) \int_{\tau_1}^{\tau_2} \cos \frac{2m\pi}{\tau_0} t' dt' + \right. \\ &\quad \left. \sin \frac{2m\pi}{\tau_0} \left(t - \frac{\theta}{\Omega} \right) \int_{\tau_1}^{\tau_2} \sin \frac{2m\pi}{\tau_0} t' dt' \right] \\ &= \frac{2F_r d\theta dr}{\pi} \sum_{l=1}^{\infty} \frac{1}{m} \left[\cos \frac{2m\pi}{\tau_0} \left(t - \frac{\theta}{\Omega} \right) \cos \frac{m\pi}{\tau_0} (\tau_2 + \tau_1) \sin \frac{m\pi}{\tau_0} (\tau_2 - \tau_1) + \right. \\ &\quad \left. \sin \frac{2m\pi}{\tau_0} \left(t - \frac{\theta}{\Omega} \right) \sin \frac{m\pi}{\tau_0} (\tau_2 + \tau_1) \sin \frac{m\pi}{\tau_0} (\tau_2 - \tau_1) \right] \\ &= \frac{2F_r d\theta dr}{\pi} \sum_{l=1}^{\infty} \frac{1}{m} \left[\cos \frac{2m\pi}{\tau_0} \left(t - \frac{\theta}{\Omega} - \frac{\tau_1 + \tau_2}{2} \right) \sin \frac{m\pi}{\tau_0} (\tau_2 - \tau_1) \right] \end{aligned} \tag{B2}$$

This expression may be written in complex form as

$$f_r(t, r, \theta) = R.P. \frac{2F_r}{\pi} \sum_{l=1}^{\infty} \frac{1}{m} e^{\frac{2im\pi}{\tau_0} \left(t - \frac{\theta}{\Omega} \right)} \left[\sin \frac{m\pi}{\tau_0} (\tau_2 - \tau_1) \right] e^{-\frac{im\pi}{\tau_0} (\tau_1 + \tau_2)} d\theta dr \tag{B3}$$

or

$$f_r(t, r, \theta) = R.P. \frac{2F_r}{\pi} \sum_{l=1}^{\infty} \frac{e^{imB(\Omega t - \theta)}}{m} \left[\sin \frac{mBb}{2r} (\mu_2 - \mu_1) \right] e^{-\frac{imBb}{2r} (\mu_2 + \mu_1)} d\theta dr \tag{B4}$$

The total force represented by $f_r(t, r, \theta)$ that acts on a blade section may be seen from equation (B1) to be

$$f_r(t, r, \theta) = F_r(\mu_2 - \mu_1)\tau d\theta dr \quad (B5)$$

If this force is to represent some preassigned percentage h_r of a total force of magnitude F , such as total thrust or total torque, that acts on the section, then

$$F_r(\mu_2 - \mu_1)\tau = \frac{h_r F}{bB} F_T \quad (B6)$$

or

$$F_r = \frac{h_r}{\mu_2 - \mu_1} \frac{r}{Bb} F \quad (B7)$$

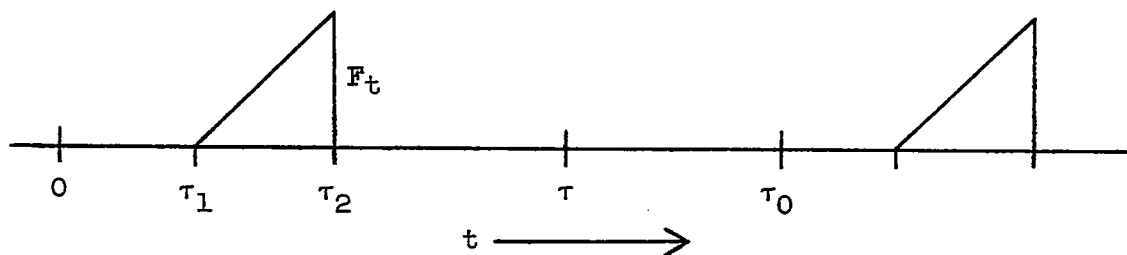
Substituting this expression for F_r into equation (B4) gives

$$f_r(t, r, \theta) = R.P. \frac{h_r F}{\pi(\mu_2 - \mu_1)} \sum_{n=1}^{\infty} \frac{2r}{mBb} e^{imB(\Omega t - \theta)} \left[\sin \frac{mBb}{2r} (\mu_2 - \mu_1) \right] e^{-\frac{imBb}{2r} (\mu_2 + \mu_1)} d\theta dr \quad (B8)$$

Note that in this equation, if $\mu_1 = 0$, $\mu_2 = 1$, and $h_r F = \frac{dT}{dr}$, the results given in equation (9) are obtained. If $\mu_1 = 0$, $\mu_2 = 1$, and $h_r F = \frac{1}{r} \frac{dQ}{dr}$, the results given in equation (10) are obtained.

Left-Triangular Element of Loading

Consider next a left-triangular element of loading $f_{lt}(t, r, \theta)$ on the chord element $\overline{\tau_1 \tau_2}$ in a time-coordinate system (see sketch).



The equation for this case may be expressed as

$$\left. \begin{array}{l} f_{lt}(t, r, \theta) = 0 \quad (0 < t < \tau_1) \\ f_{lt}(t, r, \theta) = \frac{F_t(t - \tau_1)}{\tau_2 - \tau_1} d\theta dr \quad (\tau_1 < t < \tau_2) \\ f_{lt}(t, r, \theta) = 0 \quad (\tau_2 < t < \tau_0) \\ f_{lt}(t + \tau_0, r, \theta) = f_{lt}(t, r, \theta) \end{array} \right\} \quad (B9)$$

The Fourier expansion for this function is

$$\begin{aligned} f_{lt}(t, r, \theta) &= \frac{2F_t d\theta dr}{\tau_0(\tau_2 - \tau_1)} \sum_{l=1}^{\infty} \left[\cos \frac{2m\pi}{\tau_0} \left(t - \frac{\theta}{\Omega} \right) \int_{\tau_1}^{\tau_2} (t' - \tau_1) \cos \frac{2m\pi}{\tau_0} t' dt' + \right. \\ &\quad \left. \sin \frac{2m\pi}{\tau_0} \left(t - \frac{\theta}{\Omega} \right) \int_{\tau_1}^{\tau_2} (t' - \tau_1) \sin \frac{2m\pi}{\tau_0} t' dt' \right] \\ &= \frac{F_t dr d\theta}{\pi(\tau_2 - \tau_1)} \sum_{l=1}^{\infty} \left[-\frac{\tau_2 - \tau_1}{m} \sin \frac{2m\pi}{\tau_0} \left(t - \frac{\theta}{\Omega} - \tau_2 \right) + \right. \\ &\quad \left. \frac{\tau_0}{m^2 \pi} \sin \frac{m\pi}{\tau_0} (\tau_2 - \tau_1) \sin \frac{2m\pi}{\tau_0} \left(t - \frac{\theta}{\Omega} - \frac{\tau_1 + \tau_2}{2} \right) \right] \end{aligned} \quad (B10)$$

or in complex form

$$\begin{aligned} f_{lt}(t, r, \theta) &= R.P. \frac{F_t dr d\theta}{\pi(\tau_2 - \tau_1)} \sum_{l=1}^{\infty} i e^{\frac{2im\pi}{\tau_0} \left(t - \frac{\theta}{\Omega} \right)} \left\{ \frac{\tau_2 - \tau_1}{m} e^{-\frac{2im\pi\tau_2}{\tau_0}} - \right. \\ &\quad \left. \frac{\tau_0}{m^2} \left[\sin \frac{m\pi}{\tau_0} (\tau_2 - \tau_1) \right] e^{-\frac{im\pi}{\tau_0} (\tau_1 + \tau_2)} \right\} \end{aligned} \quad (B11)$$

or

$$\begin{aligned} f_{lt}(t, r, \theta) &= R.P. \frac{F_t dr d\theta}{\pi} \sum_{l=1}^{\infty} i \frac{e^{imB(\Omega t - \theta)}}{m} \left\{ e^{-\frac{imBb}{r} \mu_2} - \right. \\ &\quad \left. \frac{2r}{mBb(\mu_2 - \mu_1)} \left[\sin \frac{mBb}{2r} (\mu_2 - \mu_1) \right] e^{-\frac{imBb}{2r} (\mu_2 + \mu_1)} \right\} \end{aligned} \quad (B12)$$

As in the preceding paragraph, if the total force acting on a blade section is to represent some preassigned percentage h_t of a total force F , then

$$F_t = \frac{2h_t r}{(\mu_2 - \mu_1)} \frac{r}{Bb} F \quad (B13)$$

and

$$f_{lt}(t, r, \theta) = R.P. \frac{h_{lt} F}{\pi(\mu_2 - \mu_1)} \sum_{l=1}^{\infty} \frac{2i r e^{imB(\Omega t - \theta)}}{mBb} \left\{ e^{-\frac{imBb}{r} \mu_2} - \frac{2r}{mBb(\mu_2 - \mu_1)} \left[\sin \frac{mBb}{2r} (\mu_2 - \mu_1) \right] e^{-\frac{imBb}{2r} (\mu_2 + \mu_1)} \right\} dr d\theta \quad (B14)$$

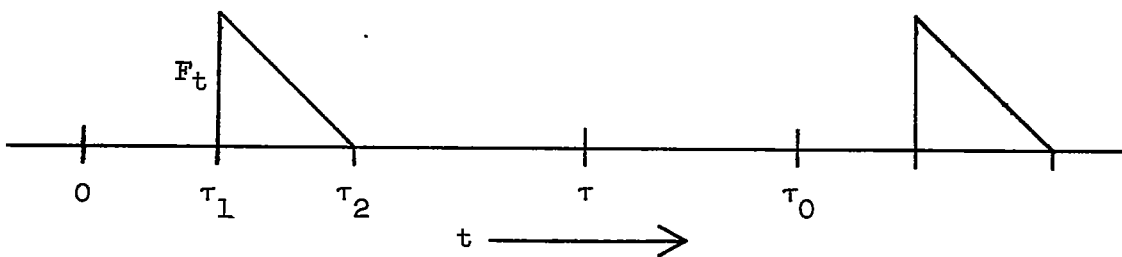
This result is easily checked by considering the limit

$$\lim_{\mu_1 \rightarrow \mu_2} f_{lt}(t, r, \theta) \quad (B15)$$

This limit leads, as it should, to the Fourier expansion of the Dirac delta function of strength $h_{lt} F$.

Right-Triangular Element of Loading

A right-triangular element of loading f_{rt} in a time-coordinate system is shown in the following sketch:



The equation for this element of loading may be written as

$$\left. \begin{array}{ll} f_{rt}(t, r, \theta) = 0 & (0 < t < \tau_1) \\ f_{rt}(t, r, \theta) = -\frac{F_t(t - \tau_2)}{\tau_2 - \tau_1} & (\tau_1 < t < \tau_2) \\ f_{rt}(t, r, \theta) = 0 & (\tau_2 < t < \tau) \\ f_{rt}(t + \tau_0, r, \theta) = f_{rt}(t, r, \theta) \end{array} \right\} \quad (B16)$$

The Fourier expansion of this equation can be obtained from equation (B14) by simply interchanging μ_1 and μ_2 . That is,

$$f_{rt}(t, r, \theta) = -R.P. \frac{h_{rt} F}{\pi(\mu_2 - \mu_1)} \sum_{l=1}^{\infty} \frac{2ire^{imB(\Omega t - \theta)}}{mBb} \left\{ e^{-\frac{imBb}{r}\mu_1} - \frac{2r}{mBb(\mu_2 - \mu_1)} \left[\sin \frac{mBb}{2r}(\mu_2 - \mu_1) \right] e^{-\frac{imBb}{2r}(\mu_2 + \mu_1)} \right\} dr d\theta \quad (B17)$$

REFERENCES

1. Gutin, L.: On the Sound Field of a Rotating Propeller. NACA TM 1195, 1948. (From Physik. Zeitschr. der Sowjetunion, Bd 9, Heft 1, 1936, pp. 57-71.)
2. Hubbard, Harvey H., and Regier, Arthur A.: Free-Space Oscillating Pressures Near the Tips of Rotating Propellers. NACA Rep. 996, 1950. (Supersedes NACA TN 1870.)
3. Garrick, I. E., and Watkins, Charles E.: A Theoretical Study of the Effect of Forward Speed on the Free-Space Sound-Pressure Field Around Propellers. NACA Rep. 1198, 1954. (Supersedes NACA TN 3018.)
4. Maynard, Julian D., and Murphy, Maurice P.: Pressure Distributions on the Blade Sections of the NACA 10-(3)(066)-033 Propeller Under Operating Conditions. NACA RM L9L12, 1950.
5. Crigler, John L., and Talkin, Herbert W.: Charts for Determining Propeller Efficiency. NACA WR L-144, 1944. (Formerly NACA ACR L4I29.)
6. Biermann, David, Gray, W. H., and Maynard, Julian D.: Wind-Tunnel Tests of Single- and Dual-Rotating Tractor Propellers of Large Blade Width. NACA WR L-385, 1942. (Formerly NACA ARR, Sept. 1942.)

TABLE I.- VALUES OF THE INTEGRAL I_1 FOR $m = 2$ (a) I_1'

$\frac{E_1}{E_2}$.4	.5	.6	.7	.75	.8	.85	.9	.925	.95	.985
0.75	0.15710177	0.26105549	0.41100003	0.63076358	0.78346608	0.98262624	1.2573318	1.6743358	1.9894793	2.1560452	3.9553356
1.0	-2.0129075	.33250404	.51680176	.78228613	.96305196	1.1946901	1.5075615	1.9707001	2.1132179	2.8116629	4.3511990
1.25	-2.105216	.60109444	.62203144	.93740778	1.1497200	1.4048845	1.7768853	2.2953038	2.6723601	3.2102575	4.8400044
1.5	.25229673	.42075982	.66046921	1.0061107	1.2440054	1.5138008	1.9120005	2.5151842	2.9860391	3.5059026	5.2166602
1.75	.39050743	.33229132	.58334111	.88276032	1.1195240	1.4260419	1.8462901	2.4561260	2.8946321	3.5115576	5.3017234
2.0	.02707319	.08785947	.21724289	.46963152	.67194751	.95100731	1.3592005	1.9756860	2.1259158	3.0718939	4.9322010
2.25	-2.4232753	-.32056899	-.34666173	-.25273869	-.12461517	.0945277	.44138211	1.0325293	1.1836002	2.1406715	4.0595015
2.5	-.50107301	-.83992925	-.10733185	-.1.201458	-.1.1802554	-.1.0644984	-.79741107	-.26916232	-.1.6882171	-.82676565	2.7957927
2.75	-.30558072	-.1.354152	-.1.085738	-.2.1821082	-.2.886475	-.2.2931330	-.2.1330769	-.1.6862412	-.1.2716711	-.61876637	1.3976334
3.0	-1.1199484	-1.7037759	-2.3435130	-2.9458572	-3.1738787	-3.3031958	-3.2602364	-2.9061165	-2.5205086	-1.8773935	.18566204
3.25	-1.1059263	-1.7355177	-2.4716596	-3.2399638	-3.5757666	-3.8223117	-3.6982677	-3.6179837	-3.2997286	-2.6711858	-5.7126580
3.5	-.80054938	-.35020280	-.2.0716911	-.2.9802607							
3.75	-.20921306	-.59466668	-.1.1666190	-.1.9901144							
4.0	.57439347	.52610994	.1.5621051	.1.5621010							
4.25	1.3781726	1.65890462	1.5820280								
4.5	1.394476	2.5601051	2.7032222								
4.75	2.1138202	2.9719568	3.3276358								
5.0	1.928725	2.7407506									
5.25	1.1373823	1.8710056									
5.5	-.01932800	.53650696									
5.75	-1.2871545	-.95808134									
6.0	-2.3570058	-2.2560971									

(b) I_1''

$\frac{E_1}{E_2}$.4	.5	.6	.7	.75	.8	.85	.9	.925	.95	.985
0.75	0.01350590	0.02110769	0.03040069	0.04138638	0.04752276	0.0507286	0.06105643	0.06845622	0.07232485	0.07629461	0.08203110
1.0	-.6592472	-.7761626	.11256662	.15317005	.17573143	.20027146	.22586666	.25774656	.28507434	.29423718	.30118765
1.25	-.3797253	.26883901	.39929448	.39372948	.45272031	.58292607	.65416161	.69174717	.73016805	.78577899	
1.5	.35474304	.39929448	.57720113	.78920538	.90826562	1.0361911	1.1731125	1.3191657	1.3956711	1.4745185	1.5888731
1.75	.11572259	.05386165	.96915744	.1.3041331	.1.5019356	1.7218360	1.9552891	2.2057833	2.3375816	2.47238367	2.6722171
2.0	.56893093	.050814006	1.3181049	1.8279065	2.1200911	2.1386913	2.1804988	2.14613416	2.35958118	2.5662409	2.86933675
2.25	.05016586	1.0433559	1.5510660	2.1899650	2.5617358	2.9800229	3.1390950	3.34650398	4.2167112	4.5014633	4.92015152
2.5	.59078093	.97799416	1.5058925	2.2083915	2.6379636	3.1272197	3.6826887	4.1911607	4.6554070	5.0206488	5.5661906
2.75	.34386349	.63341010	1.0641049	1.7574013	2.2008613	2.7296874	3.3560219	4.0930635	4.9075537	4.9552227	5.4615287
3.0	-.08958536	.00867592	.26091710	.82738301	1.219110	1.7748678	2.1469474	3.2611113	3.7689708	4.3028626	5.1145637
3.25	-.61512099	-.80519060	-.78481117	-.44598622	-.09433560	.105333810	1.1160417	2.0160253	2.6000298	3.2141225	4.4691330
3.5	-1.1983192	-1.6311761	-1.9002135	-1.8002161		-1.0621308					
3.75	-1.5901456	-2.2506842	-2.7715429	-2.9171240		-2.3189916					
4.0	-1.5716927	-2.1501125	-3.1542736	-3.51111906							
4.25	-1.3506667	-2.10469530	-2.8876947	-3.4256982							
4.5	-.63920966	-1.2211179	-1.9651593								
4.75	.35996632	.04503650	1.1611924								
5.0	1.1123142	1.1611924									
5.25	2.2595576	2.5617211									
5.5	2.9696736	3.1871242									
5.75	2.1607534	3.1188119									
6.0	1.6509401	2.3575298									

TABLE I.- VALUES OF THE INTEGRAL I_2 FOR $mB = 2$ - Continued.

(a) I_2

(d) I_a

TABLE I.- VALUES OF THE INTEGRAL, I , FOR $mB = 2$ - Concluded.

(x) \mathbb{I}_x^m

TABLE II.—VALUES OF THE INTERVAL L , FOR $m^2 = 1$.

(a) L

(b) I₁

TABLE II. - VALUES OF THE INTEGRAL I_v FOR $mB = 3$ - Continued(c) I_2^*

$K_1 \backslash K_2$.4	.5	.6	.7	.75	.8	.85	.9	.925	.95	.985
0.75	0.05167710	0.13830183	0.20868877	0.359567078	0.56951923	1.3037751	2.9518675	3.5420125	4.9720678	7.6246195	21.129987
1.0	.05600960	.12897922	.2725978	.57002133	.83798787	1.2651280	2.0058310	3.1873459	4.9126573	7.5001280	21.350163
1.25	.03695842	.08993033	.20486552	.6212267	.70405803	1.1036666	1.8113136	3.2559668	4.6610505	7.2975013	21.053356
1.5	.01775337	.01763323	.01754393	.16193115	.33365836	.65084647	1.2450790	2.6035098	3.9505394	6.5153197	20.188633
1.75	.-1.2841970	.-2.2904197	.-1.15437786	.-1.1107892	.-1.1637169	.-2.7080592	.-1.1530295	.1.2562097	2.41775563	4.9082023	18.376778
2.0	.-2.7293978	.-5.2931110	.-1.49502710	.-1.3110388	.-1.5519840	.-1.5865071	.-1.6010225	.-8.7800390	.-1.2562510	2.3213028	15.432252
2.25	.-1.0227996	.-8.0793025	.-1.1321943	.-2.3009219	.-2.8072307	.-3.3080120	.-3.6729606	.-3.1097566	.-2.8136282	.-9.5689360	11.597535
2.5	.-1.0519833	.-8.66495377	.-1.6161161	.-2.8599995	.-3.4369193	.-4.5366280	.-5.1140835	.-5.9170151	.-5.6389593	.-4.2513402	7.5617961
2.75	.-1.18591216	.-5.15359821	.-1.2164205	.-2.5315687	.-3.5094779	.-4.1177087	.-6.1020586	.-7.3807173	.-6.7417081	.-6.105777	
3.0	.-2.6614805	.-2.7769344	.-0.0533185	.-1.1306893	.-2.1387153	.-3.5391662	.-5.3591151	.-7.3800161	.-8.1374856	.-8.0068238	1.6215291
3.25	.-7.9808806	.-1.2719201	.-1.5260091	.-1.9834373C	.-1.3015204	.-1.305061	.-1.4521450	.-6.2412536	.-7.6072611	.-8.2750198	.-11.3646590
3.5	1.1209501	1.9893943	2.8870939	3.0211396							
3.75	.96259820	1.9362598	3.1882959	4.0658265							
4.0	.22780871	9.1332840	2.2057470	3.7118321							
4.25	.-8.5504971	.-7.7727911	.-2.0493433	.-2.1375417							
4.5	.-1.7693293	.-2.3793992	.-1.9512570								
4.75	.-1.9692786	.-3.0670035	.-3.2651613								
5.0	.-1.1772851	.-2.3840428									
5.25	.-3.6141496	.-5.8260602									
5.5	1.9412866	1.5539667									
5.75	2.7316872	2.9149492									
6.0	2.2634650	2.9868839									

(d) I_2^*

$K_1 \backslash K_2$.4	.5	.6	.7	.75	.8	.85	.9	.925	.95	.985
0.75	0.05047470	0.1086098	0.21122800	0.40611651	0.56579407	0.79463387	1.117742h	1.7520035	2.2540958	3.0533840	5.9305802
1.0	.08012192	.17093011	.33336201	.62622677	.85970133	1.1945962	1.7039619	2.5620393	3.2634512	4.3699899	8.2085942
1.25	.-1.2272871	.-2.5929565	.-5.0185020	.-9.2958815	.-1.2615754	.-1.7379866	.-2.4449863	.-3.6111183	.-4.5477418	.-6.0013482	11.0185149
1.5	.-1.1739948	.-3.62914462	.-7.0054866	.-1.937716	.-1.7513280	.-2.3996474	.-3.3467679	.-4.8865001	.-6.1010265	.-7.9407185	14.237196
1.75	.-1.9576852	.-4.2387133	.-8.3635452	.-1.5790083	.-2.1668030	.-2.9880205	.-4.2038867	.-6.1551995	.-7.6819503	.-9.3935699	17.612005
2.0	.-1.3157766	.-2.2233068	.-7.4035411	.-1.5280739	.-2.1837708	.-3.1361919	.-4.5779383	.-6.9311307	.-8.7826546	.-11.379337	20.624580
2.25	.-0.29111597	.-0.25028660	.-2.1704531	.-8.7180075	.-1.4624639	.-2.4477557	.-4.0058232	.-6.6771982	.-8.8213822	.-12.081096	22.623622
2.5	.-3.1760431	.-5.2394858	.-6.6915469	.-4.6136665	.-4.0847987	.-7.7417689	.-2.2829966	.-5.1193711	.-7.5012401	.-11.199696	23.251147
2.75	.-6.1750439	.-1.1862066	.-1.7228662	.-2.1246130	.-2.0468616	.-1.9501530	.-2.27505372	.-2.5439252	.-5.0813804	.-9.1516968	22.787186
3.0	.-7.6151252	.-1.1592311	.-2.4415103	.-3.4436132	.-3.8132186	.-3.7525005	.-2.8765303	.-2.97226050	.-2.3298508	.-6.7055854	21.753790
3.25	.-5.2327961	.-1.1896125	.-2.3063999	.-3.8115042	.-4.1522219	.-4.1900671	.-4.7886881	.-4.1152112	.-4.05933990	.-4.6131058	21.069327
3.5	.-0.05304669	.-1.2033278	.-1.1012232	.-2.7768025							
3.75	.-8.0509217	1.1605162	.-8.2623226	.-6.6811186							
4.0	1.41810777	2.3279832	2.6794502	1.6065330							
4.25	1.1628350	2.6104877	3.5663275	3.1544097							
4.5	.-6.6096266	1.4951365	3.0132385	1.2501676							
4.75	.-6.7775399	.-1.6867328									
5.0	.-1.9354605	.-2.1086051									
5.25	.-2.4111855	.-3.1954691									
5.5	-1.7213102	.-2.4570637									
5.75	.-0.0976269	.-1.2509208									
6.0	1.7019760	.-8.20000180									

TABLE II.- VALUES OF THE INTEGRAL I_1 FOR $mB = 3$ - Concluded.

(a) L_x

(r) Σ

TABLE III.- VALUES OF THE INTEGRAL I_1 FOR $mB = 4$ (a) I_1'

$K_1 \backslash K_2$.4	.5	.6	.7	.75	.8	.85	.9	.925	.95	.985
0.75	0.00682117	0.01838656	0.01368909	0.09785398	0.1469437	0.22047526	0.36215192	0.56293125	0.75364012	1.0675619	2.2513744
1.0	.01190926	.03195520	.07288285	.15731575	.29919744	.33594001	.50255039	.78783773	1.0521427	1.3928923	2.7009490
1.25	.01763814	.04681605	.10926373	.23577920	.34209692	.45725597	.73253305	1.1183389	1.4216636	1.8032889	3.3738767
1.5	.01066880	.03160974	.08617382	.21515902	.33060684	.51557880	.80204693	1.2006386	1.6559772	2.2137968	3.9320784
1.75	.03340448	.07016378	.11199858	.11793643	.07571059	.03851174	.26114778	.72262393	1.1181127	1.7311178	3.4379687
2.0	.11034726	.25819132	.50005482	.80128910	.14621315	.18728325	.97933174	-1.09665215	-1.1026511	-0.8529732	-0.3553637
2.25	.15152561	.38097135	.81439368	.53251719	.125311559	.17901904	-2.4390113	-2.6647027	-2.7932762	-2.6181101	-2.8115685
2.5	.19483673	.16439368	.53251719	.125311559	.18672507	.23639736	-0.89403619	-1.7715111	-3.788767	-3.7548692	-3.5169658
2.75	.22116512	.10304661	.48966921	.16966921	.16672507	.23639736	-0.23639736	-2.4995462	-3.0276153	-3.0526132	-1.4621626
3.0	.16627685	.99908540	1.6601007	2.3665262	1.9498861	1.4707215	.55112393	.72218012	-1.3544439	-1.7352558	-0.6978505
3.25	.36472587	.92733070	1.8118090	2.8118943	3.0411851	2.7693218	2.0832126	.481114322	-0.4853110	-1.2363477	-0.70962078
3.5	.20351646	.11595393	1.6929591	1.6819239	.44660486	1.5474676					
3.75	.87116821	-1.6929591	-1.6819239	-1.81979712							
4.0	.95390520	-1.9331618	-2.7539361	-2.3369458							
4.25	.09781615	.71110966	.71042679	-1.9680071							
4.5	1.1671769	1.1041372	.63232713								
4.75	1.6811570	2.0312505	2.2001650								
5.0	.7172h939	1.6805776									
5.25	-1.1139911	-0.6759292									
5.5	-2.2808119	-2.1063250									
5.75	-1.4933171	-2.0900559									
6.0	.72h94344	-2.2295391									

(b) I_1''

$K_1 \backslash K_2$.4	.5	.6	.7	.75	.8	.85	.9	.925	.95	.985
0.75	0.00035723	0.00047349	0.00161283	0.00336276	0.004413396	0.00574326	0.00732482	0.00921279	0.01081309	0.01144497	0.01323h85
1.0	.00336277	.00823142	.01712012	.03183267	.04203110	.05453171	.06965578	.08776056	.09046417	.10922804	.12617098
1.25	.01516684	.03810556	.07970549	.11917861	.19770606	.25746775	.33025710	.41790956	.46795544	.52251117	.60720269
1.5	.011414101	.10309942	.21857714	.31592544	.55610503	.71102030	.94680599	.12103685	.13621550	.15294661	.17904895
1.75	.04938995	.16562158	.36513076	.72179549	.9912167	1.3736396	1.7689178	2.1164120	2.4611375	3.0065637	3.5114h13
2.0	.03517587	.11055713	.2930100	.69211514	1.0218012	1.4809127	2.10818178	2.9411342	3.4622471	4.0571216	5.0369805
2.25	.08661186	.16460486	.21006466	.90001166	.13446194	.5233853	1.1655311	2.1572560	2.8266055	3.6366330	5.0495153
2.5	.28757524	.55207222	.96570959	-1.4042812	-1.6287175	-1.3688317	-0.5127522	.00317613	.75297527	1.7365969	3.5970047
2.75	.26974276	.6591865	-1.3575597	-2.2744687	-2.7052850	-2.9716562	-2.6715621	-2.1073488	-1.3373170	-2.1164763	2.1218969
3.0	.00623245	.11957700	.63755688	-1.61413681	-2.0112225	-2.8211968	-3.1078560	-2.6674731	-1.9589310	-1.77236330	1.9982907
3.25	.14151063	.051414725	1.02146067	.18191075	.13075718	.92611298	-1.6461167	-1.1742304	-1.2569344	-1.73116603	2.8125219
3.5	.73360780	1.5200911	2.3857311	2.4699696							
3.75	.31162711	.587719530	2.0038153	2.7310283							
4.0	.59690746	.66568078	.05096769	1.0885009	1.7181005						
4.25	.13212920	.21600812	.2036503	-1.0601776							
4.5	.96894070	.24257469	.26219976								
4.75	.16166554	.09695377	-1.0601776								
5.0	.17953145	.2039434									
5.25	.17829524	.25933872									
5.5	.10911860	.56338606									
5.75	.1.9634988	-1.2586121									
6.0	.2.206969	-2.1896321									

TABLE III.—VALUES OF THE INTEGRAL, I, FOR $nB = 4$ —Continued.

(c) I

(a) L

TABLE III. - VALUES OF THE INTEGRAL I_1 FOR $mB = 4$ - Concluded.(e) I_1'

$K_1 \backslash K_2$.4	.5	.6	.7	.75	.8	.85	.9	.925	.95	.985
0.75	0.01661833	0.05268302	0.15463967	0.45772183	0.81115150	1.5169372	3.0688027	7.1906959	12.269533	24.190046	128.58068
1.0	-0.0057349	.0574270	.0122539	.19750351	.41963260	.90993350	2.0988086	5.5574640	10.042300	20.962891	121.42597
1.25	-0.02668224	-0.0782118	-0.1573665	-0.22193089	-0.20717910	-0.37646510	-0.62569230	3.1263873	6.7804592	16.327116	111.58966
1.5	-0.07537638	-0.19593710	-0.3731611	-0.66951829	-1.1667076	-1.4715153	-1.5682380	-0.1051110	2.1090222	9.8223950	98.306896
1.75	-0.1805125	-0.3125518	-0.80010683	-1.7056526	-2.4258096	-3.3780180	-4.5123096	-5.1671154	-4.1530815	1.1727680	81.204008
2.0	-0.4121903	-0.1217962	-1.0337092	-2.3908454	-3.5652120	-5.2061452	-7.8149956	-10.556768	-11.135686	-9.1081130	40.578703
2.25	-0.05274885	-0.2612730	-0.71335600	-2.2598306	-3.7236792	-6.0371119	-9.6548624	-15.057984	-18.139069	-19.362286	37.592123
2.5	-0.17839388	.30587063	.2395664	.73828700	.2.0926079	.1.4016305	.9.0936050	-16.856335	-22.208566	-27.162324	15.593651
2.75	-0.34653832	.99751281	1.7185187	1.9261102	1.1996998	.88109030	-5.5602595	-15.139441	-22.828398	-32.261192	-5.2557710
3.0	-0.8704211	1.2198904	2.6926999	4.3631088	4.9711907	3.6611359	.31033690	-10.810161	-20.131676	-31.053028	-24.581339
3.25	-0.9485769	.82042717	2.0915370	4.8320456	6.2875370	8.8255082	1.4060077	-5.6836857	-16.610565	-31.038417	-43.088858
3.5	-0.62085985	-.08095068	-.21322623	2.5616663	7.3082207						
3.75	-1.1230915	-2.2353666	-2.8987797	-.95266612	5.5912712						
4.0	-0.30403990	-2.1772889	-3.9931468	-3.8260818							
4.25	-0.36653467	-.33131770	-2.5206788	-4.5288359							
4.5	1.63771429	2.1468259	5.8371578								
4.75	1.78556625	3.3000173	3.0399217								
5.0	3.7929119	2.0373758									
5.25	-1.667931	-.78040124									
5.5	-2.6270747	-2.9681916									
5.75	-1.4768679	-2.96822661									
6.0	1.0406009	-.96575664									

(f) I_1''

$K_1 \backslash K_2$.4	.5	.6	.7	.75	.8	.85	.9	.925	.95	.985
0.75	0.03899175	0.112164	0.29071793	0.73372689	1.1829557	1.9629577	3.4367638	6.6734225	10.013419	16.575692	53.916411
1.0	0.05110966	.11066951	.364680170	.97283907	1.5700690	2.6079407	4.5704368	8.8829048	13.394493	22.062291	71.866978
1.25	0.09706665	1.7392586	1.45761320	1.1727046	1.9054175	3.1857035	5.6161663	10.983990	15.534391	27.053025	89.661078
1.5	0.05126411	1.15853769	J.4405850	1.2103952	2.0252797	3.4823481	6.3046819	12.627130	19.221005	32.251659	106.78773
1.75	0.01166098	0.03986201	2.1041875	.82718750	1.5308836	3.0350222	6.0245927	13.030566	20.509806	35.477677	122.06984
2.0	-.10330261	-.24365876	-.37030401	-.25254317	-.17655080	1.2914653	4.0152937	11.156085	19.195270	35.736600	133.803037
2.25	-.21524566	-.60052228	-.1.2071167	-.1.9591600	-.2.1659662	-.1.8366555	-.01167180	6.41597439	11.568581	32.060015	140.62530
2.5	-.29113099	-.79149112	-.1.2066781	-.3.5348091	-.4.5784918	-.5.6030918	-.5.0514767	-.27313300	7.1942749	21.869503	142.52756
2.75	-.101613309	-.45261792	-.1.4578688	-.3.7132761	-.5.5310920	-.7.608762	-.9.1783745	-.7.0120694	-.9.0735620	15.900993	140.83452
3.0	.33190290	.50015961	.15546384	.1.8101815	.3.9257617	.6.9942175	.10.578722	-.11.780809	-.7.0016714	7.1627030	136.89820
3.25	.71100938	1.5591726	2.3337276	1.6996681	-.2.2329220	-.3.711708	-.9.0802628	-.14.019582	-.12.854725	-.9.6650500	130.87657
3.5	.60704837	1.7917751	3.5029194	5.5146199	6.8538690	3.7011819					
3.75	-.04448302	-.60845118	2.4795127	5.1359429							
4.0	-1.0688867	-.1.1634329	-.3.9726755	3.1639307							
4.25	-1.5136637	-.2.817766	-.3.2137788	-.11768458							
4.5	-.7390387	-.2.2818129	-.3.9767612								
4.75	.94900628	.18612675	-.2.2954036								
5.0	2.2127638	2.7261067									
5.25	1.6013004	3.1324292									
5.5	-.24691874	1.5292540									
5.75	-.2.3732315	-.1.2024732									
6.0	-.2.7239276	-.2.7917235									

TABLE IV.—VALUES OF THE INTEGRAL, I , FOR $\alpha^2 = 6$

(a) L'

(b) x_1^n

TABLE IV.- VALUES OF THE INTEGRAL I_2 FOR $m_b = 6$ - Continued(e) I_2'

$K_2 \setminus K_1$.4	.5	.6	.7	.75	.8	.85	.9	.925	.95	.985
0.75	0.00056369	0.00267235	0.01073420	0.04070362	0.08022855	0.16339915	0.35461375	0.87357610	1.4993684	2.8951402	12.779896
1.0	.00044752	.00222868	.00940457	.03733079	.07510994	.15583318	.34388754	.85812277	1.4111321	2.3746744	12.753148
1.25	-.00079358	-.00256030	-.00510592	-.0010671	.01825775	.07124272	.22067072	.68266400	1.2734680	2.6292661	12.445585
1.5	-.00622969	-.0203913	-.07199203	-.17890308	-.25667981	-.34511653	-.39953454	-.21296189	.2097280	1.3501690	10.820226
1.75	-.01133765	-.00211667	-.19517613	-.51180231	-.60160470	-.11094500	-.10216337	-.1.8924970	-2.5062509	-2.6151356	-2.0953335
2.0	-.00211667	-.02611369	-.1180231	-.51180231	-.60160470	-.1.1094500	-.1.9507888	-.3.2725118	-.5.160560	-.6.2116156	-.6.8913105
2.25	.05088354	.16589592	.37200094	.47204377	.24670694	.46911813	.2.0139086	-.4.9706748	-.7.0722580	-.9.3161965	-.6.5130061
2.5	.05580563	.16589592	.37200094	.47204377	.24670694	.46911813	.2.0139086	-.4.9706748	-.7.0722580	-.9.3161965	-.6.5130061
2.75	-.47404761	-.13066485	.10285691	.1.3372170	.2.5228738	.3.8735859	.4.5761718	2.6676628	-.3.6713717	-.7.6975010	-.9.1600751
3.0	-.23047569	-.75302347	-.1.5997031	-.1.8011119	-.94855242	-.85676687	3.1280323	3.1995919	1.25943561	-.4.0570811	-.11.856675
3.25	.02223873	-.30158572	-.1.4320388	-.3.2058538	-.3.4330390	-.2.2150503	-.2.3900973	-.1.9132330	.06843866	3.9264405	3.2160796
3.5	.47572251	1.1581323	1.35940289	1.59030322							
3.75	.26287137	1.1818080	2.7115591	2.3396338							
4.0	-.70473760	-.1.0895296	.03906069	1.8938723							
4.25	-.76361130	-.2.1586316	-.2.61113950	1.8938723							
4.5	-.75772230	.35843862	-.1.6009299	1.96117958							
4.75	1.4222595	2.61710582	-.95527100								
5.0	-.49519105	.72934260									
5.25	-.2.0308423	-.2.1313977									
5.5	-.09933082	-.1.4471899									
5.75	2.3282231	.88969015									
6.0	.86171220	1.19914011									

(a) I_2''

$K_2 \setminus K_1$.4	.5	.6	.7	.75	.8	.85	.9	.925	.95	.985
0.75	0.00078032	0.00351754	0.01319068	0.04533337	0.08444626	0.15958700	0.31471801	0.67777530	1.0593331	1.7965822	5.4380306
1.0	.00155362	.03692604	.02476365	.06197189	.11626798	.27233426	.51928432	1.0768680	1.6052756	2.7176105	7.6128562
1.25	.00329169	.01396611	.01616897	.15753901	.27747507	.49311551	.90300606	1.7732163	2.6602637	4.1573224	11.037324
1.5	.00137997	.01831166	.07011666	.23915195	.43181811	.78021377	1.4357860	2.7881940	4.0475915	6.2511867	15.411385
1.75	-.00614453	-.01718495	-.02273798	-.05706805	.21362901	.51009682	1.3530576	4.0395768	7.8285718	19.748779	
2.0	-.03066667	-.11440680	-.32265236	-.69507121	-.89431196	-.96932674	-.62123681	.92257260	2.7796697	6.3120667	21.093360
2.25	-.02480591	-.12397278	-.46068531	-.1.3394690	-.2.0764336	-.2.9758972	-.3.7521077	-.3.4566381	-.2.0733555	1.3966050	18.346021
2.5	-.05802082	.18309894	.25139406	-.24281777	-.1.0422507	-.2.4227744	-.4.3411243	-.5.9396710	-.5.607086	-.3.0101744	15.389657
2.75	1.3628275	.50366880	1.3002331	2.2146570	2.2060527	1.3090391	.96547834	4.3785958	-.5.5860475	-.4.5820524	13.454694
3.0	-.05655071	.04235969	.69132968	2.4726631	.5.3038449	3.8502796	2.3616589	2.0355545	4.779075	-.5.9435527	10.4117897
3.25	-.34701514	-.98958110	-.1.6515138	-.78949139	-.69177200	2.4077681	2.8017761	-.81778582	-.4.4743016	-.7.7233127	5.9009733
3.5	-.10126976	-.69785069	-.2.1693376	-.3.1860290							
3.75	.60151321	1.2051303	.75376792	-.1.5370268							
4.0	.48546033	1.6947694	2.8893501	.93788635							
4.25	-.76368263	-.79859323	-.33412345	1.3698524							
4.5	-.1.0437602	-.2.40599397	-.1.9183142								
4.75	.67066962	-.18374710	-.1.5985615								
5.0	1.7592655	2.4990062									
5.25	-.2.2316066	1.1616585									
5.5	-.2.2333642	-.1.5692611									
5.75	-.4.7694015	-.1.6602340									
6.0	2.2963554	.20708553									

TABLE IV. - VALUES OF THE INTEGRAL, I_n , FOR $nB = 6$ - Concluded

(a) L₃

(f) \mathbf{L}_g^{\star}

K_1	.4	.5	.6	.7	.75	.8	.85	.9	.925	.95	.965
K_2											
0.75	0.00251676	0.01207837	0.04867170	0.18358195	0.36166040	0.73623020	1.59800680	3.93300662	6.7101792	13.036251	57.512699
1.0	-0.00345663	-0.01590103	-0.06400996	-0.24322265	-0.17905838	-0.97015970	2.12565668	5.2369090	8.9909255	17.370495	76.671108
1.25	-0.00317785	-0.01516558	-0.06021316	-0.2056644	-0.28016788	-0.56317557	1.1687794	2.5780955	6.43507716	11.107199	21.550182
1.5	-0.00116558	-0.00021316	-0.02239332	-0.17381163	-0.12691510	1.02770010	2.54649056	6.9315878	12.387082	24.758996	111.36561
1.75	-1.1707624	-0.06390402	-0.17782691	-0.35116942	-0.30226585	-0.15992710	-0.92691590	5.0675394	10.804213	28.490163	125.61093
2.0	-0.03120309	-0.11531061	-0.19161910	-0.3086208	-0.19165537	-0.7905121	-3.1116637	-0.82049610	4.0871212	17.718213	130.87251
2.25	-0.00180394	-0.05655112	-0.07233806	-0.15645320	-0.28701092	-0.48938688	-7.5295555	-8.9505383	-6.4256967	5.0356900	124.59970
2.5	-0.10181522	-0.32084267	-0.6565200	-0.37157718	-0.68655390	-3.1304232	-7.6634715	-13.712721	-18.969264	-8.0913061	112.93006
2.75	-1.1719174	-0.51675996	-1.5983895	-3.2762818	-3.63685825	-2.10279993	-2.2265734	-12.175335	-17.715757	-17.701817	97.529803
3.0	-1.13668661	-1.19515192	-0.43314665	3.0117101	5.0557612	6.3271478	3.9369987	-7.2865062	-17.077206	-24.732718	77.432622
3.25	-3.6917833	-1.18112268	-2.2192455	-1.22650162	1.3038220	4.9952931	6.7774732	-1.8285693	-13.877263	-29.096605	58.070627
3.5	-0.10738249	-0.51177632	-0.44168213	-4.3715100	-1.2505513	-1.8925112					
3.75	-0.59512336	-1.58482091	1.09463690	-2.6560292	-	-					
4.0	-0.02802891	-1.7601186	3.5327177	-0.87555957	-	-					
4.25	-0.37179580	-1.10175695	1.2284376	2.5732160	-	-					
4.5	-1.0497041	-2.7688293	-2.2299249	-	-	-					
4.75	-0.8139020	-1.5764969	-2.1023451	-	-	-					
5.0	1.8239083	-2.1326804	-	-	-	-					
5.25	-1.1179109	-1.5139386	-	-	-	-					
5.5	-2.4034374	-1.6901470	-	-	-	-					
5.75	-2.6667135	-1.9699491	-	-	-	-					
6.0	2.1668880	-10.313628	-	-	-	-					

TABLE V - VALUES OF THE INTEGRAL I_1 FOR $mB = 8$ (a) I_1'

$K_1 \setminus K_2$.4	.5	.6	.7	.75	.8	.85	.9	.925	.95	.985
0.75	0.00001616	0.00011571	0.00026397	0.00032219	0.00052132	0.01428270	0.03263820	0.09193012	0.13912320	0.25870569	0.92995562
1.0	.00005287	.00036023	.00183717	.00799168	.01422639	.03212735	.04899000	.15418311	.261427950	.41618335	1.2109382
1.25	.00007480	.00072281	.00320105	.01140168	.01848009	.03803402	.07713855	.15837384	.33512557	.50493907	.79599866
1.5	-.00059220	-.00321045	-.01140168	-.02756115	-.03223108	-.03889807	.01611625	.24903522	.51251433	.95470490	2.5166153
1.75	-.00319398	-.01275367	-.01972911	-.02151053	-.03737639	-.06032376	-.09013763	-.1.15276791	-.1.1519691	-.90016373	.83613620
2.0	.00135866	.01960505	.01220271	-.01059503	.01851226	-.05180332	-.1.2720169	-.2.3735257	-.2.98914891	-.3.4441604	-2.5181235
2.25	.01631453	.046588028	.02193555	.05232454	1.2435206	1.5131297	1.4213708	.37727768	.60273141	-.1.7581722	-2.1263927
2.5	-.02496885	-.12961625	-.02235282	-.01091680	.058995325	1.1618432	2.04495873	2.5049316	1.7180806	.23687612	-1.5797227
2.75	-.02158859	-.17195119	-.075466003	-.1.8886166	-.2.2741286	-.1.9984911	-.76589480	.69131508	.70375508	-.40400554	-3.1277588
3.0	-.10812720	.02929131	.05568117	.33716567	.55582031	.1.3486500	1.0403251	.96341207	1.8686836	1.5677817	-1.6586802
3.25	-.02571724	.14313818	1.0056642	2.2957071	1.9891244	.62275301	-.70461984	-.02096971	1.1686257	1.5998363	-1.3640851
3.5	-.25942691	-.1.0212137	-.1.4626387	-.1.7515848	-.1.1515848	1.21141891					
3.75	.27815509	.16715697	.05813052								
4.0	-.31339693	.1.103695	2.1822120	-.07042040							
4.25	-.79192782	-.1.5036858	-.32939780								
4.5	.02211123	-.87147766	-.1.0836252								
4.75	1.2058116	2.1530113	-.01675111								
5.0	-.1.0725793	-.32334320									
5.25	-.81594036	-.1.4778693									
5.5	1.9757196	.70461654									
5.75	-.11391770	.35536380									
6.0	-.1.803846	.27589809									

(b) I_1''

$K_1 \setminus K_2$.4	.5	.6	.7	.75	.8	.85	.9	.925	.95	.985
0.75	0.00000048	0.000000210	0.00000702	0.00001464	0.00001309	0.00001256	0.00011835	0.00010812	0.00023376	0.00029017	0.00036839
1.0	.00001607	.00009760	.0001612	.000147302	.00257665	.0035152	.00712592	.01135623	.01120270	.01766234	.02375049
1.25	.00020658	.00127280	.00568113	.02036295	.032036295	.03610865	.06217515	.10461618	.21253932	.26697116	.36394796
1.5	.00057754	.00391885	.01975205	.01975259	.15045863	.27142519	.48516803	.83588779	.1.0617379	.1.1047639	.1.9939463
1.75	-.00160939	-.00765775	-.02111943	-.01615686	-.03379163	-.1.7759950	-.5113738	1.2363799	1.6304012	2.0512012	4.3366514
2.0	-.00497007	-.03205136	-.1.2695717	-.1.48130538	-.1.7901388	-.1.0510949	-.1.2639916	-.99275208	-.1.4466162	.58756120	3.3135311
2.25	.01132091	.04710974	.09610219	-.05535851	-.39791251	-.1.0630161	-.2.05118869	-.2.99131048	-.3.0616350	-.2.1383155	.72476314
2.5	.01726376	.11758400	.50103518	.1.3590096	.1.6123863	.1.976855	.2.0555336	-.3.11334940	-.1.1512545	-.1.3601706	1.4925547
2.75	-.05735784	-.23056495	-.66646164	-.095731024	-.65771057	1.6311292	2.1102961	.93255979	-.36140018	-.5168911	.73155668
3.0	-.01305174	-.19763880	-.97563150	-.2.2636113	2.3046095	-.1.5715519	-.00456167	.52683329	-.38431706	-.1.8657160	-.95388700
3.25	.17339217	.70561190	.3.3681397	.62315580	-.36209561	-.58900761	-.32223099	2.0673190	1.6117862	.21764067	-.25671261
3.5	-.11664222	-.05012187	.92070260	.1.8932800							
3.75	-.31332504	-.1.2930058	-.2.1926061	-.54211319							
4.0	.51210068	.93121561	-.05875013	-.36090512							
4.25	.18924595	1.2781077	1.7135856	-.8910543							
4.5	-.1.0534216	-.1.9650377	-.36118947	-.37361220							
4.75	.53146065	-.217577802									
5.0	1.158765	3.4585768									
5.25	-.1.6022303	-.70295778									
5.5	-.28972271	-.811489248									
5.75	2.0052406	3.2236321									
6.0	-.1.0925946	.15077187									

TABLE V.- VALUES OF THE INTEGRAL I_y FOR $mB = 8$ - Continued

(a) L_2

(d) L_2'

TABLE V - VALUES OF THE INTERVAL L_0 FOR $mB = 8$ - Concluded

(e) L₅

(r) L₃

TABLE VI.—VALUES OF THE INTEGRAL, L , FOR $mB = 9$

(a) L_1'

(b) \mathbf{I}_1

TABLE VI.- VALUES OF THE INTEGRAL I_1 FOR $mB = 9$ - Continued(c) I_2^1

$K_1 \backslash K_2$.4	.5	.6	.7	.75	.8	.85	.9	.925	.95	.985
0.75	0.0000577	0.00005135	0.00039715	0.00277236	0.00738632	0.02043796	0.06125758	0.21519182	0.45170119	1.0990559	7.5136291
1.0	0.0000481	0.0000527	0.00030510	0.00239223	0.06656721	0.1911384	0.09008013	0.21138267	0.46805843	1.09290443	7.5149055
1.25	-0.0000577	-0.00042124	-0.0211579	-0.0770631	-0.1253095	-0.1975234	-0.0308061	0.10186636	-0.3087050	-0.91187610	7.3237106
1.5	-0.00036907	-0.00300285	-0.01715106	-0.0761004	-0.11975106	-0.27965020	-0.19301945	-0.77684157	-0.8617908	-0.63734390	5.0599732
1.75	0.00022369	-0.0002576	-0.01280167	-0.1146107	-0.26857437	-0.44988310	-0.15215716	-2.9388099	-0.0271642	-5.1999307	-2.1161788
2.0	0.0019777	0.02629946	0.1737726	0.05639465	0.50050403	1.2201220	2.10168550	0.01619201	-2.29711112	0.4777521	-7.8317287
2.25	-0.00197390	-0.18112046	-0.01735134	-0.17504886	-1.7375404	-1.0959372	1.1912560	3.5125123	1.4863974	-3.0974114	-10.828847
2.5	-0.1329523	-0.11121849	-0.5102522	-0.45392012	-1.82147371	-3.3127225	-2.9772269	1.5102363	1.3671762	-7.3122260	-15.201890
2.75	0.191281	0.20453807	0.1387048	-0.45392012	2.7136979	0.74578095	-2.1115172	3.5287323	3.7223954	-15.360252	
3.0	0.1137485	0.10951673	0.09846940	0.27861664	-0.70206516	1.7263460	1.8782472	-0.65839012	6.4666668	-12.985961	
3.25	-0.12120618	-0.09165649	-0.17197691	-0.18257790	-2.1577602	1.1192863	-1.3090372	-3.8765369	-0.6321945	5.2420797	-11.043181
3.5	0.21349466	0.51161621	0.68815352	2.1220405	0.87767415	1.0610955	0.57089408				
3.75	0.00325102	0.16104450	-1.7943263	-1.8303153	-1.610172	1.3106752					
4.0	0.16104450	-1.7943263	-1.8303153	-1.610172							
4.25	0.6771839	0.87774930	0.65518170	0.76106505							
4.5	0.10833380	1.3947224	0.95518170								
4.75	-1.1217723	-2.2105250									
5.0	1.6112215	0.55498135									
5.25	-1.7668517	1.1934911									
5.5	-0.6111983	-7.3815042									
5.75	2.0217719	-5.2100711									
6.0	0.10484583	0.0990585									

(d) I_2^2

$K_1 \backslash K_2$.4	.5	.6	.7	.75	.8	.85	.9	.925	.95	.985
0.75	0.00000813	0.00009645	0.00069956	0.00136899	0.01082766	0.02716559	0.07374693	0.22310215	0.42215678	0.89361600	4.1630667
1.0	0.0002851	0.0024636	0.00146159	0.09474600	0.02810555	-0.05012118	0.1368432	0.3810668	0.70587124	1.4299290	6.1513702
1.25	0.0006289	0.0072182	0.0072182	0.06569045	0.02523345	0.07004655	0.12926922	0.3083361	0.77163650	1.3189311	2.4711953
1.5	-0.0006285	-0.00030395	-0.00212714	-0.02312714	-0.02312714	0.06996779	0.19205771	0.50851246	1.3726128	0.3130603	4.2707095
1.75	-0.0012504	-0.0962833	-0.0962833	-0.0962833	-0.0962833	-0.18379906	-0.30596935	-0.43615864	-1.02532127	0.28300529	1.4421713
2.0	0.0012182	0.0227955	-0.02716559	-0.02716559	-0.02716559	-0.28591515	-0.68783614	-1.45261311	-2.6705956	-3.92461222	-2.0181612
2.25	0.0790151	0.0630532	0.28521353	0.82396710	1.05404657	0.82402708	-0.59994390	-3.9471269	-5.98139582	-6.7805116	8.0792751
2.5	-0.1612730	-0.07392717	-0.09376356	-0.62067108	1.6884876	3.1672637	3.9875735	1.4639670	-1.93359501	-5.8305139	4.3820270
2.75	-0.01254320	-1.5155862	-0.83504618	-2.2964668	-2.1312719	-1.19646143	1.6682030	2.91190111	.297665605	-4.840162	-2.0820116
3.0	0.0227431	0.4009621	1.0021971	0.06820634	-1.5379600	-2.7065251	-0.89002956	3.8235677	3.8400009	-1.6661257	-5.6336906
3.25	-0.0822657	-1.1707250	-0.80273903	2.770859	2.2246034	-4.2973305	-2.4360896	1.7881873	0.5226162	1.5897560	-9.783532
3.5	-1.1150614	-0.85928375	-2.3405377	-0.95308280	-1.3885886	0.96022250	2.7121137				
3.75	0.37737092	1.23907269	0.77966846	-1.3885886	-1.30364642						
4.0	-2.7660788	0.05839493	1.8645530	-0.50594775	1.3303642						
4.25	-0.36698125	-1.91130882	-1.5379600								
4.5	1.0408677	1.6231797	-0.56516203	-0.9919247							
4.75	-0.76133463	-1.0333532									
5.0	-0.71387541	-1.9427471									
5.25	1.8597532	0.97834542									
5.5	-1.2505726	-0.57308379									
5.75	-0.74834524	-0.2846176									
6.0	2.0997690	-0.97161517									

TABLE VI.- VALUES OF THE INTEGRAL I_0 , FOR $mE = 9$ - Concluded.

(e) I_3

(f) Σ_3

TABLE VII.—VALUES OF THE INTEGRAL, I, FOR $\epsilon B = 12$

(a) I_1

(b) L

TABLE VII.—VALUES OF THE INTEGRAL I_1 FOR $nB = 12$ —Continued.

{□} L₂

(4) x_2

TABLE VII.- VALUES OF THE INTEGRAL I_1 FOR $mB = 12$ - Concluded(a) I_1

$K_1 \backslash K_2$.4	.5	.6	.7	.75	.8	.85	.9	.925	.95	.985
0.75	0.00150244	0.00000698	-0.00003785	-0.00043850	-0.00016686	-0.00243409	0.00015630	0.07161210	0.31259540	1.5230303	36.589500
1.0	-0.01877477	-0.00020358	-0.00022902	-0.00237917	-0.00737662	-0.0280195	-0.07110260	-0.21608620	-0.32944620	-1.11738420	25.505794
1.25	.00193758	-0.00048804	-0.00059395	-0.00926478	-0.02752227	-0.06207686	-0.25380360	-0.85038020	-1.6261938	-3.1208991	8.4090400
1.5	-0.0170727	.00022213	-0.00069023	-0.01729294	-0.06176410	-0.20769280	-0.68668130	-2.3611837	-4.5844554	-9.4170711	-20.079508
1.75	.00132851	.00185667	-0.01819417	-0.01709875	.24136933	.38666390	.23119510	-2.0075341	6.0068759	-15.960324	-61.124294
2.0	-0.0103582	-0.00580427	-0.02937621	-0.02824898	.35822144	1.3990343	3.7890021	6.7141847	5.4402609	-5.0153981	-89.269229
2.25	.00057574	.00193173	-0.07131060	-0.01687666	-1.8099412	-2.7195422	-1.89331669	6.3972631	13.232304	13.394711	-94.467711
2.5	.00196774	.03652050	.36751827	1.5785286	1.7031527	-1.3785270	-5.5956990	-1.8398840	5.1998045	21.056131	-81.469588
2.75	-0.1118300	-1.3984672	-0.7879674	-0.78999795	1.3990215	4.5592161	2.2787934	-8.9670486	-6.3180202	16.30061	-53.416775
3.0	.03337407	.29973763	.80065400	-1.6890336	3.2184644	-1.1711804	5.4444838	-3.3924589	-12.767854	2.1567441	-16.730129
3.25	-0.0687775	-1.11934810	.031172975	-1.4612213	1.2674961	-3.7603684	.42746030	5.5777822	-8.9586036	-13.167817	20.381027
3.5	.11828607	.32443884	-1.5057555	-1.4612213	-1.6914392	.89319308					
3.75	-1.14479126	.11835267	2.5759285	2.0567274	3.6445108						
4.0	.10233837	.86791460	-2.1641889								
4.25	.066265575	1.8572848	.36317064								
4.5	-1.39846934	.2383617	1.3126965								
4.75	.87949887	2.385869	-1.6140954								
5.0	-1.4184852	-.99610276									
5.25	1.4601949	-.26457552									
5.5	-2.0324624	1.0141181									
5.75	1.8213323	-.61800617									
6.0	-1.2411918	-.11185914									

(e) I_3

$K_1 \backslash K_2$.4	.5	.6	.7	.75	.8	.85	.9	.925	.95	.985
0.75	0.00125279	0.00000797	0.00012161	0.00167876	0.00609266	0.02898114	0.09516060	0.47705170	1.246394	3.7535859	40.446386
1.0	-0.0057106	.00020268	.00018750	.00224834	.00069114	.03051957	.12657270	.63512010	1.6319507	5.0735151	53.526217
1.25	-.00091804	-.00002768	-.00009187	-.00074731	-.00524758	.08721202	.13474900	.75911670	1.9713348	6.1583348	67.255203
1.5	.000916192	-.00042765	-.00137665	-.03114399	-.07176410	-.16077315	-.279595870	-.07222160	.95299210	5.3437057	77.314548
1.75	-.00144796	.00061844	-.00013657	-.05526890	-.20948211	-.66722710	-.1.8679230	-.4.4875294	-.6.0911305	-.5.3391347	68.302223
2.0	.000205777	.04163679	-.05083461	.30833175	.77189330	.1.1855179	.57337470	-.4.6101305	-.11.238222	-.21.593731	31.573977
2.25	-.003560134	-.02313824	-.16843562	-.41530318	-.05860628	1.6671779	5.5217023	7.4575590	1.5871174	-.16.46872	-.9.3295860
2.5	.007045055	.05183110	.15351833	-.72651655	-.2.1907586	-.4.6832452	-.3.1371499	7.4574111	11.057947	-.2.3780113	-.69.634384
2.75	-.011652716	-.01973693	-.26836151	2.5814912	3.463769	1.3652015	-.23682360	-.2.3682360	11.825315	11.371915	-.77.330006
3.0	.01118570	-.06571804	-.1.1719209	-.2.9154844	-.70701394	3.4501860	-.8.9690060	-.9.0869240	20.751660	21.371915	-.91.881111
3.25	-.00899278	.37512768	2.0007057	.57122838	-2.5706113	-.53340259	6.0384738	-.6.6020738	-.9.1252855	16.712114	-.89.389720
3.5	-.07228674	-.86886324	-.2.1250818	1.9314278		-.1.3640844					
3.75	-.19949303	1.3712109	.90669322	-.1.2041794							
4.0	-.39573402	-.1.5723359	.80310610	-.1.8492310	2.7130606						
4.25	-.62907197	1.2091139	-.1.5041313								
4.5	-.82400977	-.30189827	-.74625359	-.43304230							
4.75	.87811786										
5.0	-.69508254	1.3230712									
5.25	-.24297860	-.1.030432									
5.5	-.10444096	-.09556318									
5.75	-.1.0658367	1.3099952									
6.0	1.5035955	-.1.8308635									

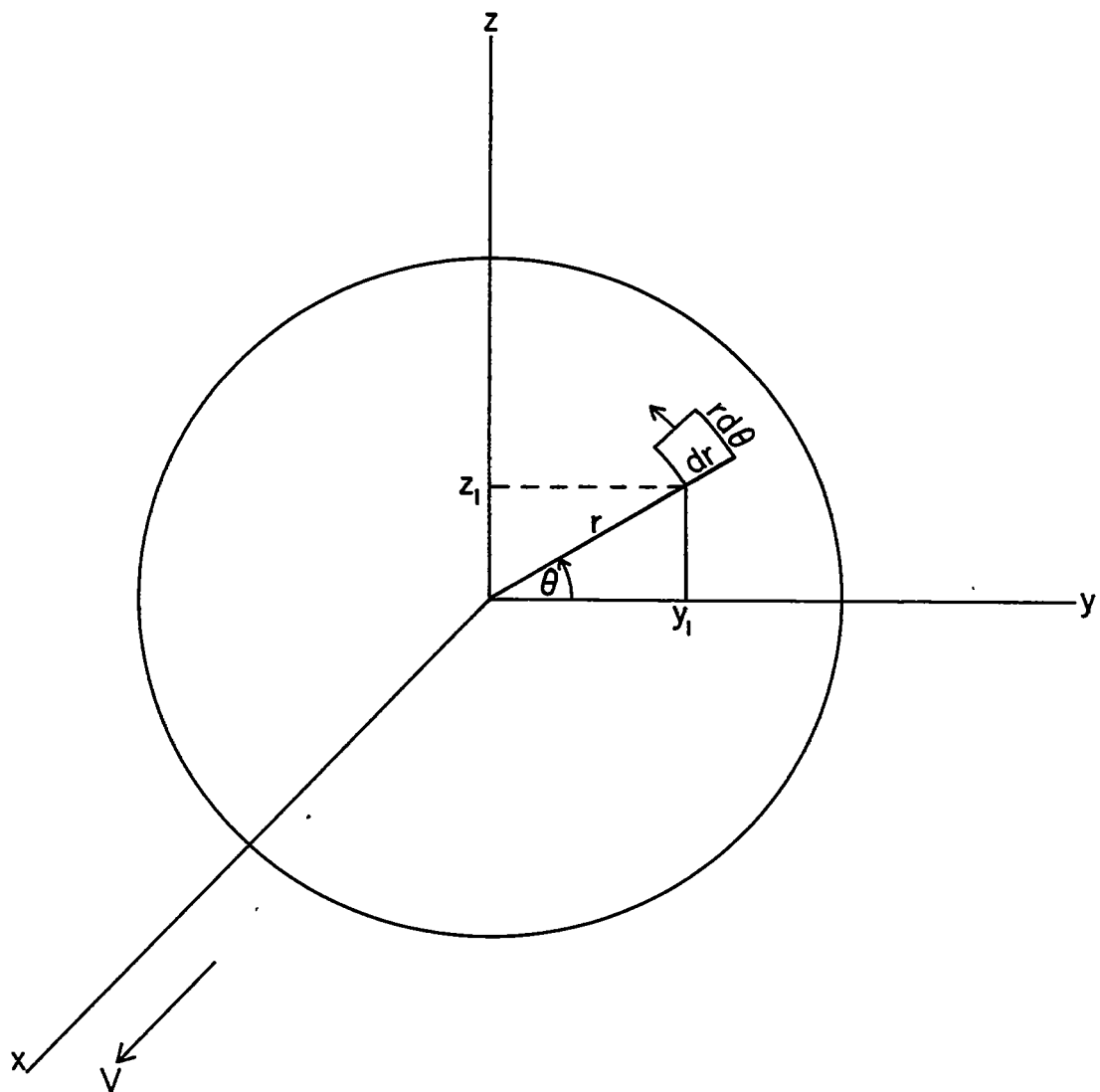


Figure 1.- Propeller disk and coordinate system.

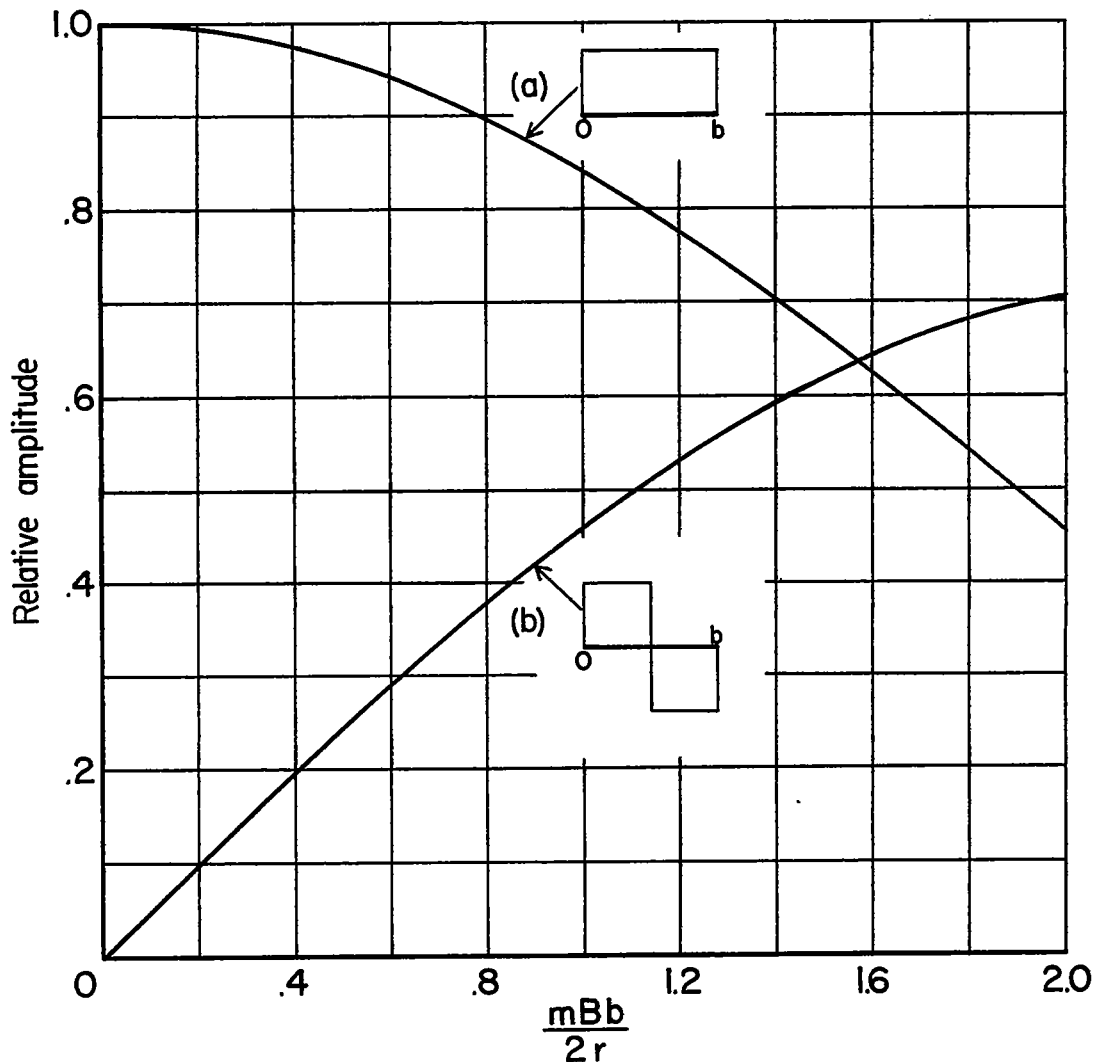
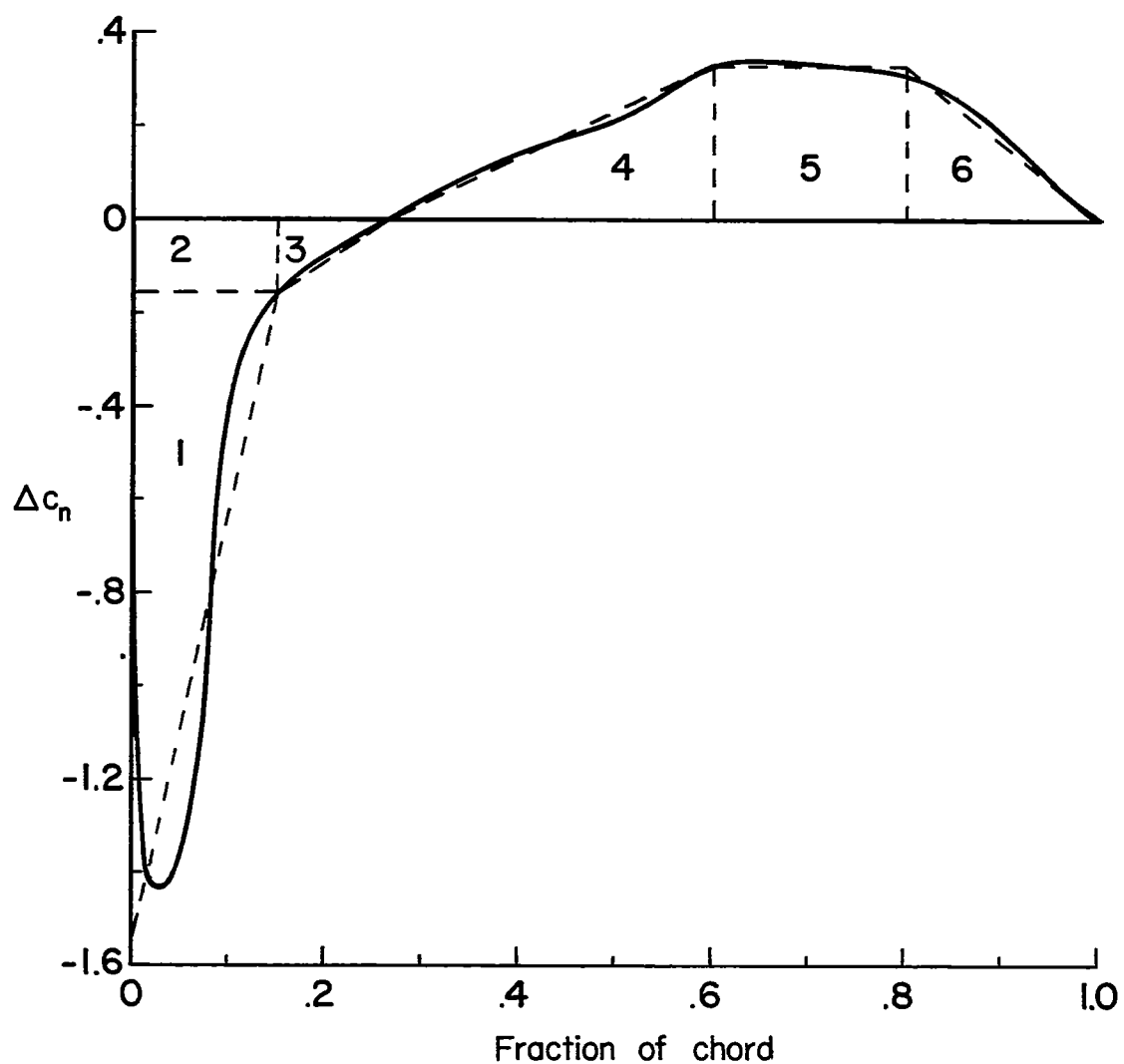
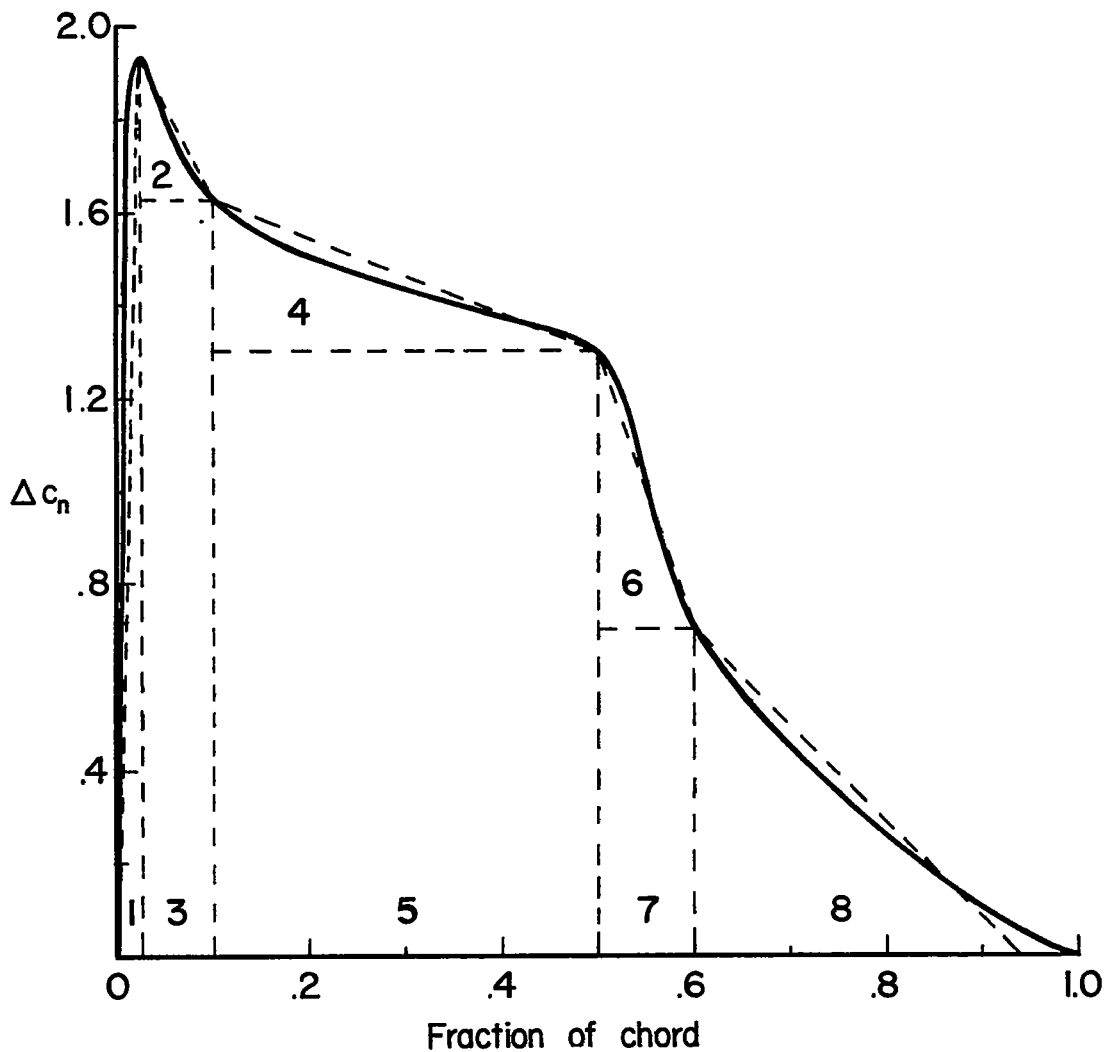


Figure 2.- Relative amplitude functions, (a) $\frac{2r}{mBb} \sin \frac{mBb}{2r}$ and
(b) $\frac{4r}{mBb} \sin^2 \frac{mBb}{4r}$, plotted as functions of $\frac{mBb}{2r}$.



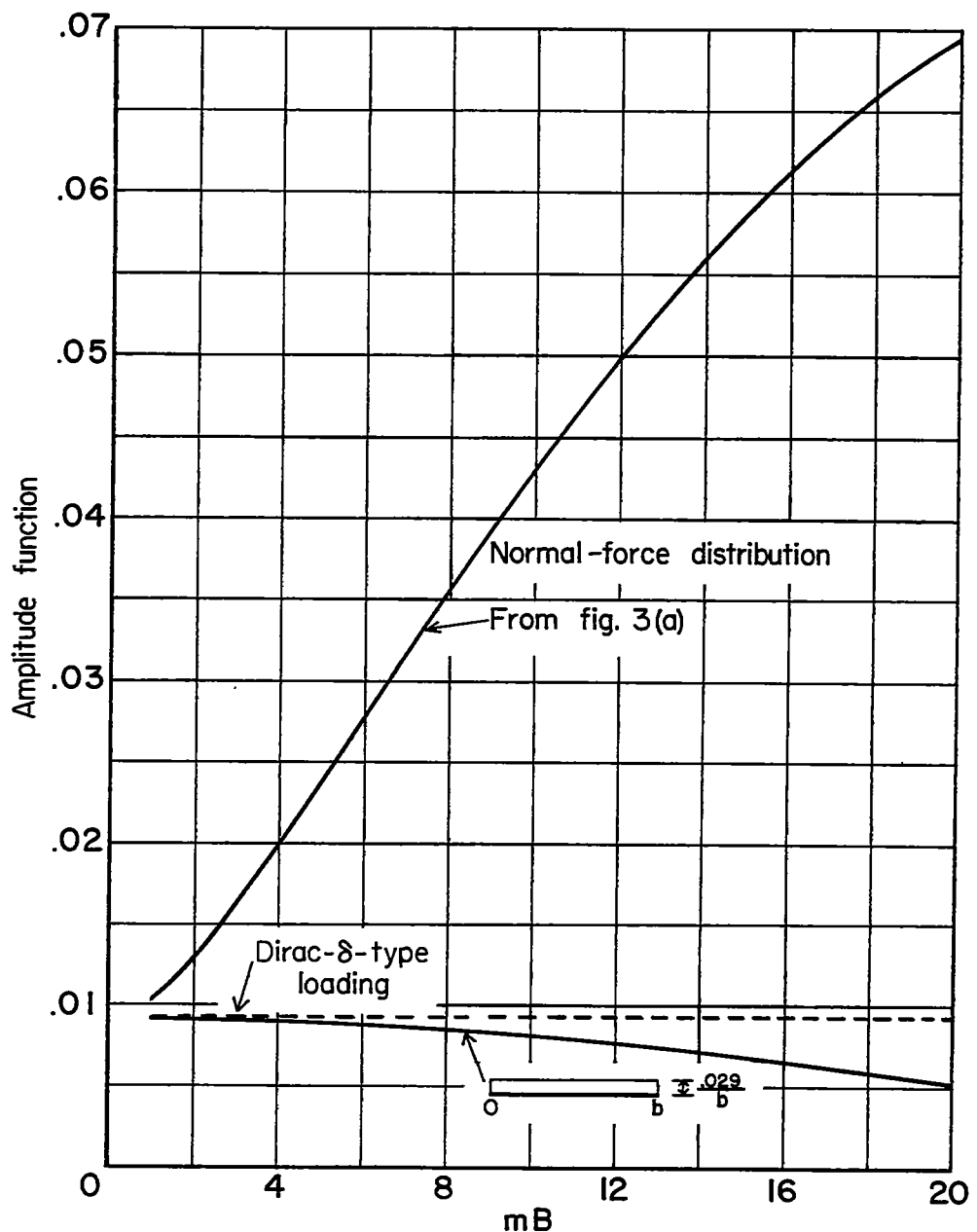
(a) $c_n = 0.029$; $J = 2.55$; $M_r = 0.8$; $n = 1,500$ rpm; $\beta_{0.75R} = 45^\circ$.

Figure 3.- Chordwise normal-force distribution at $0.78R$ for two sets of operating conditions (ref. 4). (Numbers indicate rectangles and triangles used for the analysis.)



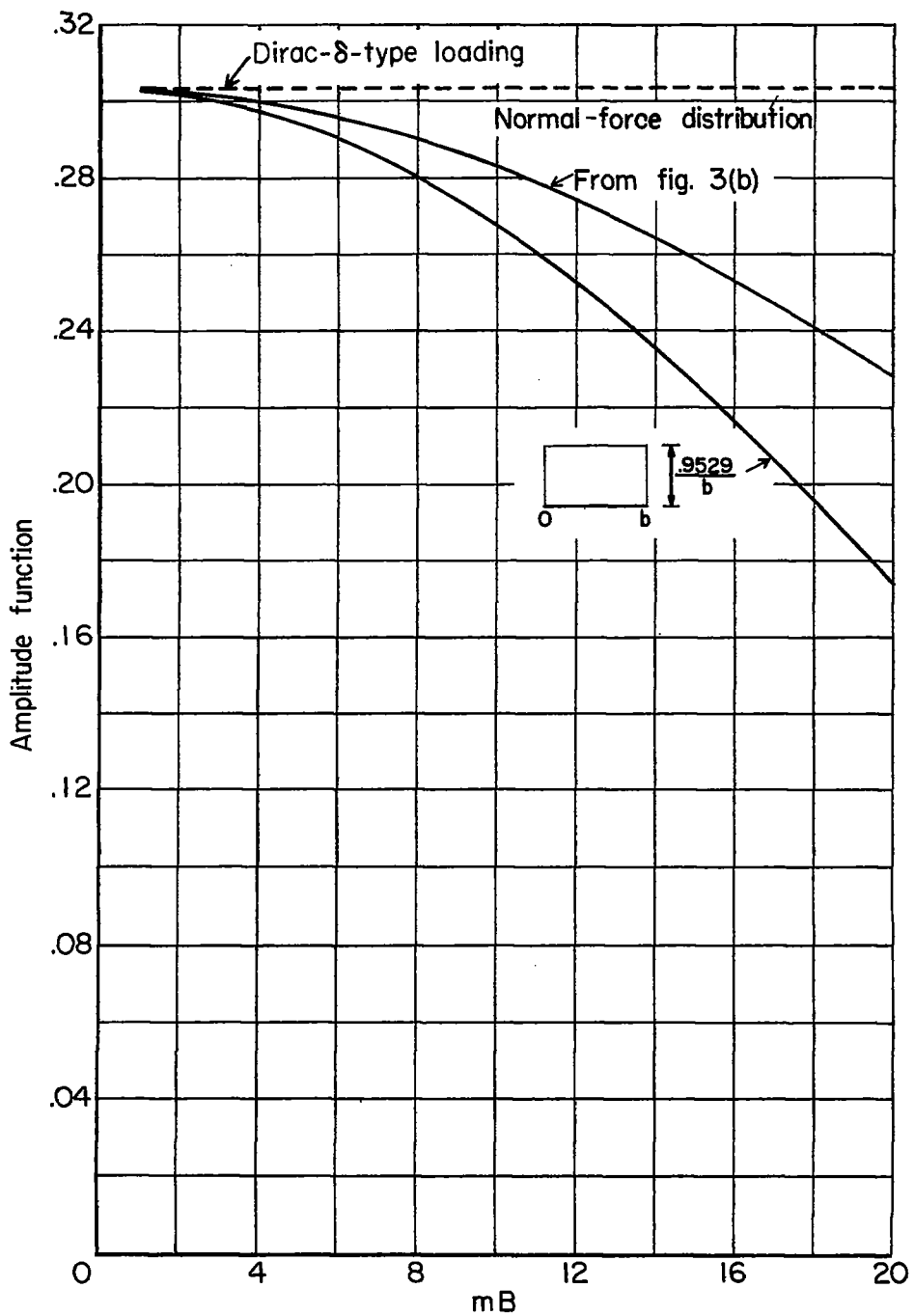
(b) $c_n = 0.9529$; $J = 1.009$; $M_r = 0.789$; $n = 2,000$ rpm; $\beta_{0.75R} = 30^\circ$.

Figure 3.- Concluded.



(a) $c_n = 0.029$; $J = 2.55$; $M_r = 0.8$; $n = 1,500$ rpm; $\beta_{0.75R} = 45^\circ$.

Figure 4.- Amplitude functions associated with the normal-force distributions in figure 3 plotted as functions of mB compared with amplitude functions associated with uniform distributions of normal force.
 $b/r = 0.1715$.



(b) $c_n = 0.9529$; $J = 1.009$; $M_r = 0.789$; $n = 2,000$ rpm; $\beta_{0.75R} = 30^\circ$.

Figure 4.- Concluded.

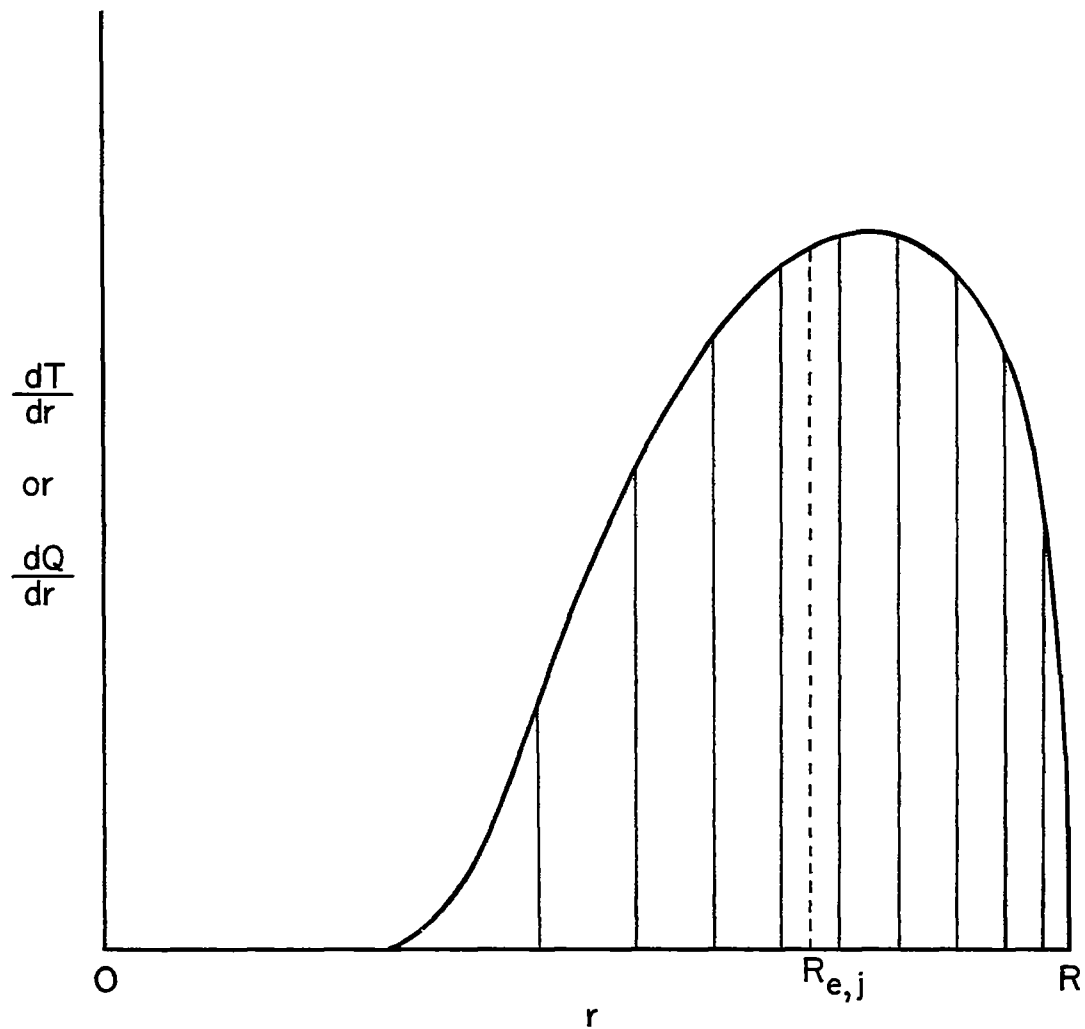
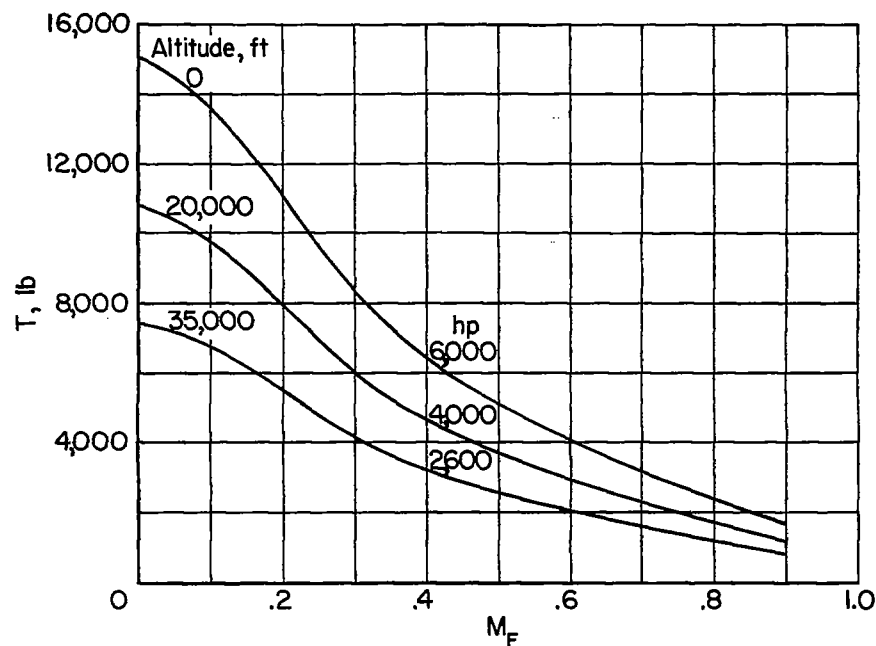
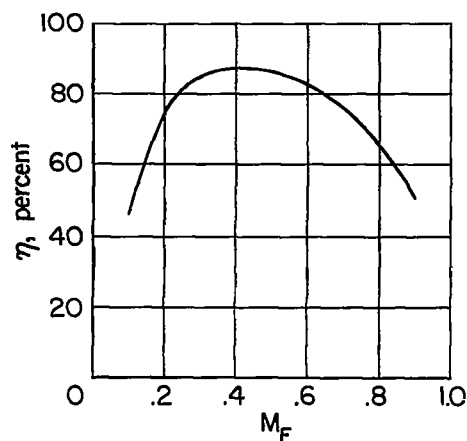


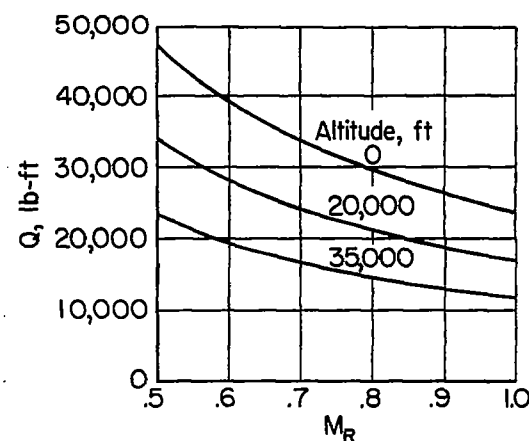
Figure 5.- Sketch of radial thrust or torque distribution.



(a) Thrust.

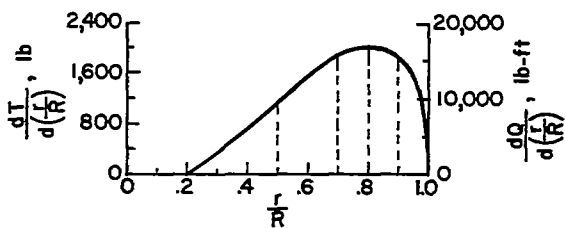


(b) Efficiency.



(c) Torque.

Figure 6.- Efficiency, total thrust, and total torque for various operating conditions for a 16-foot-diameter propeller.



Radial distribution of thrust and torque (per blade)

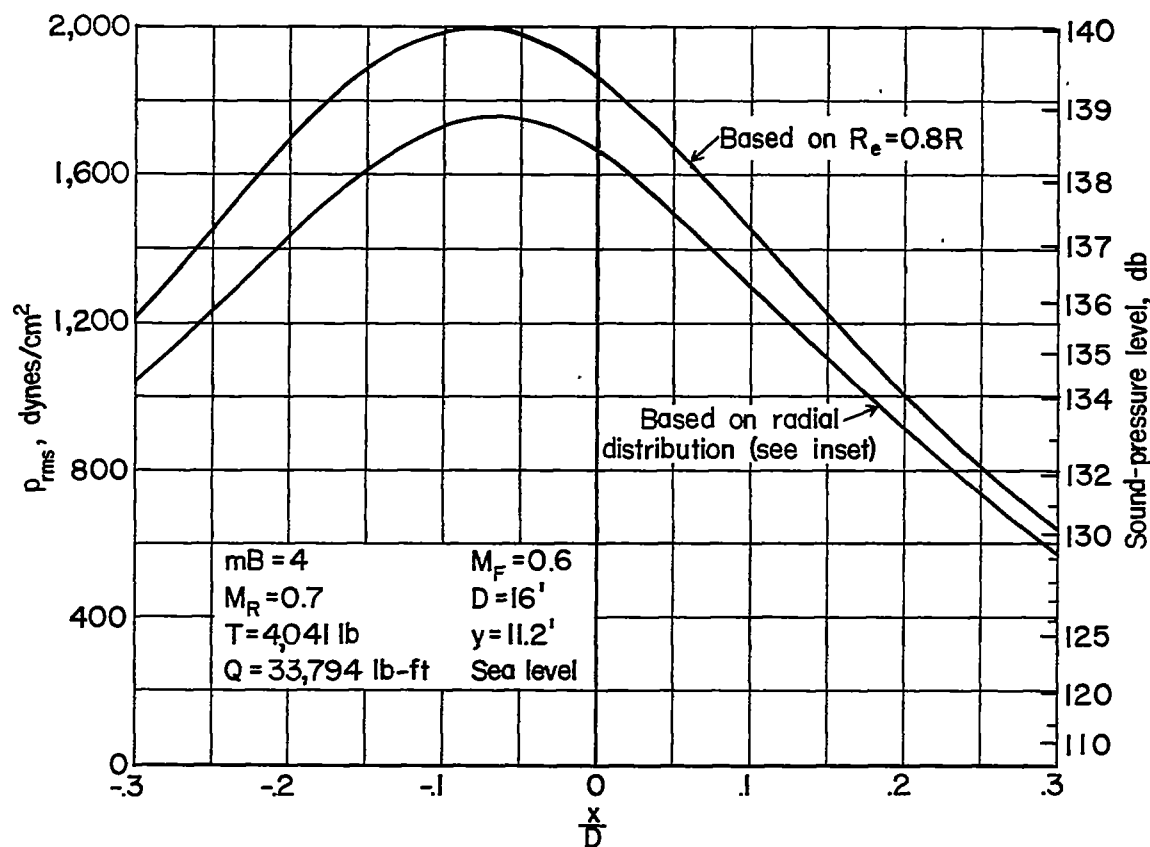


Figure 7.- Comparison of sound-pressure calculations for forces concentrated at an effective radius with calculations for forces distributed along the propeller radius.

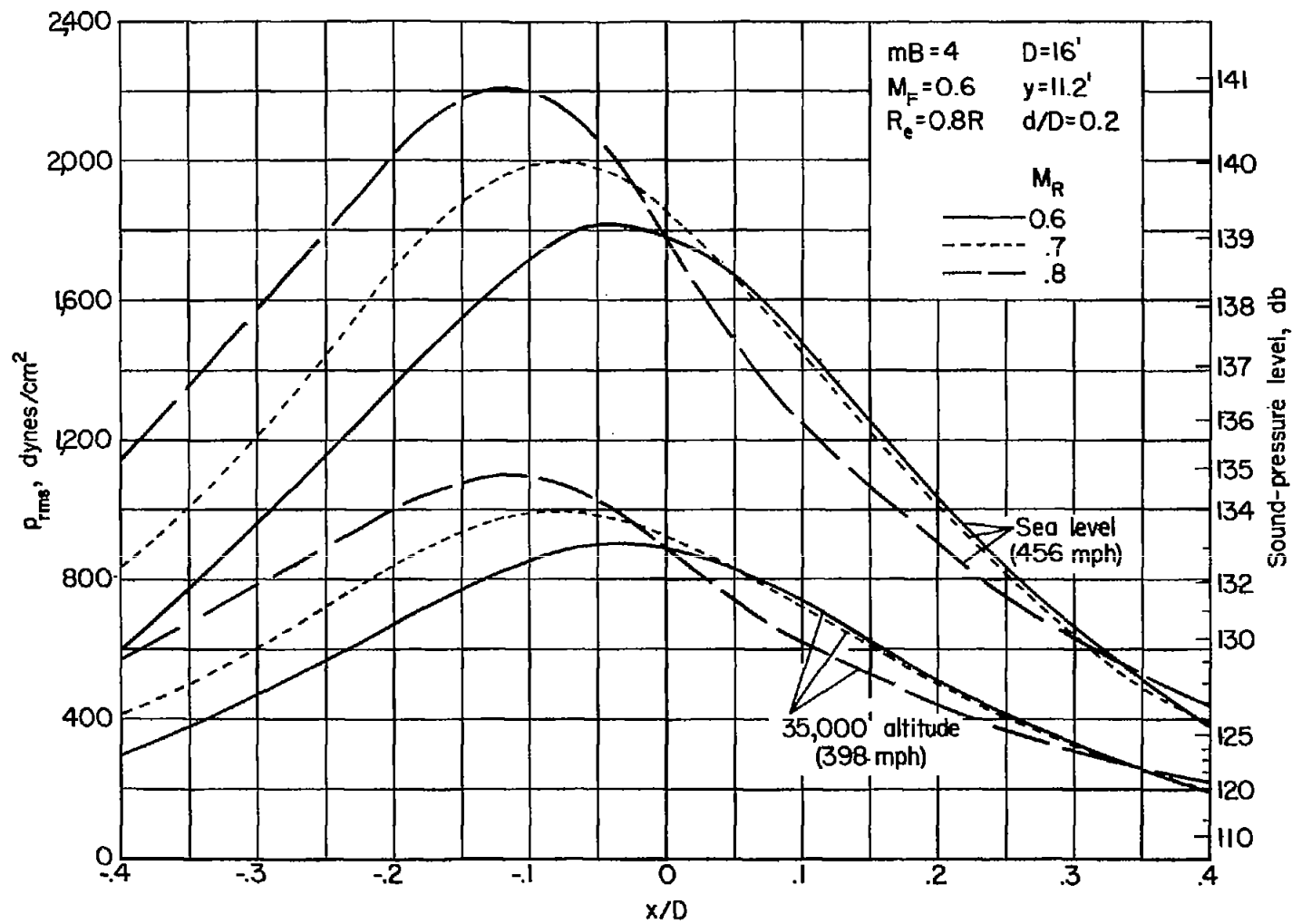


Figure 8.- Distribution of the root-mean-square pressures for the first harmonic of a four-blade 16-foot-diameter propeller at two altitudes and several tip Mach numbers.

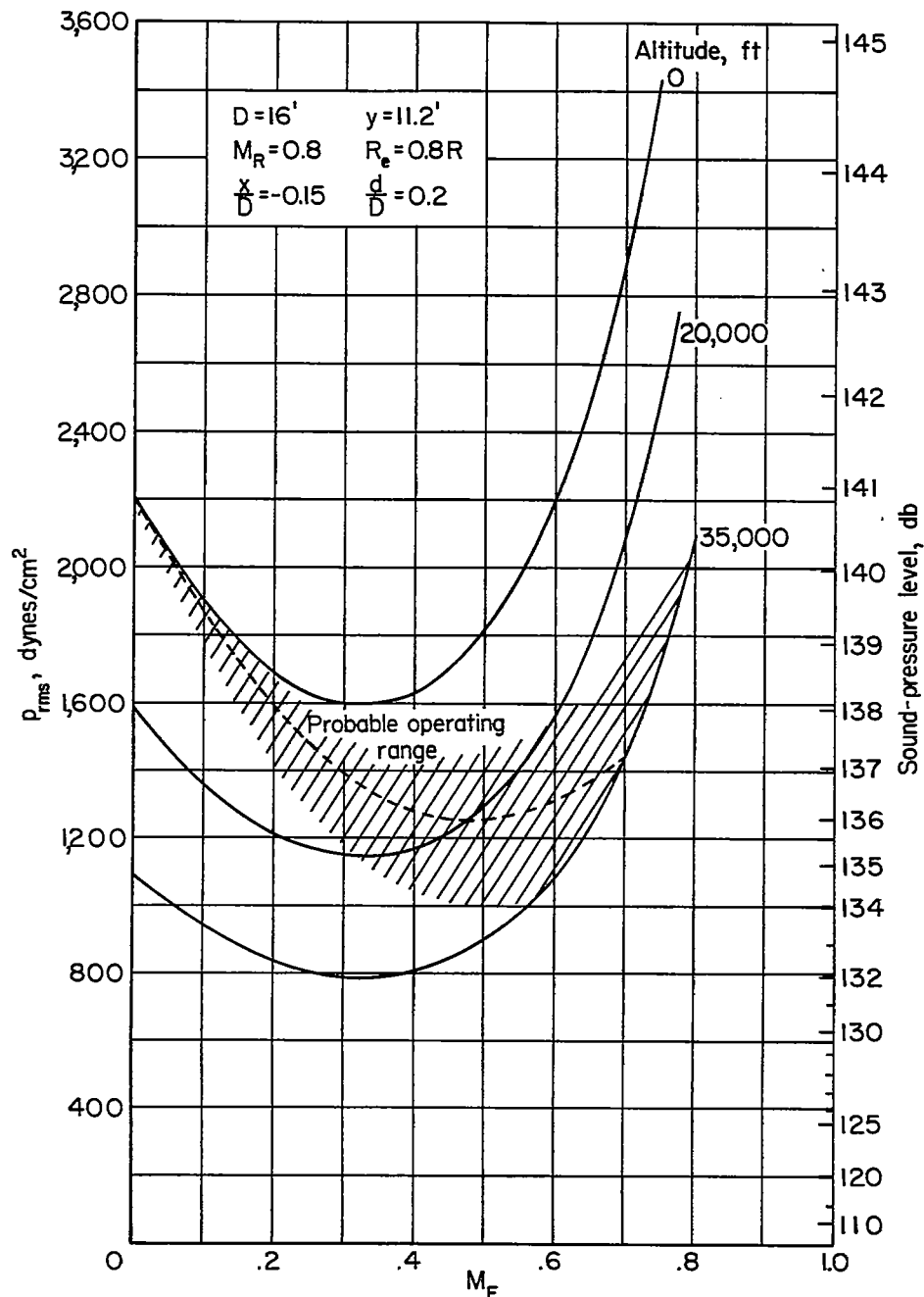
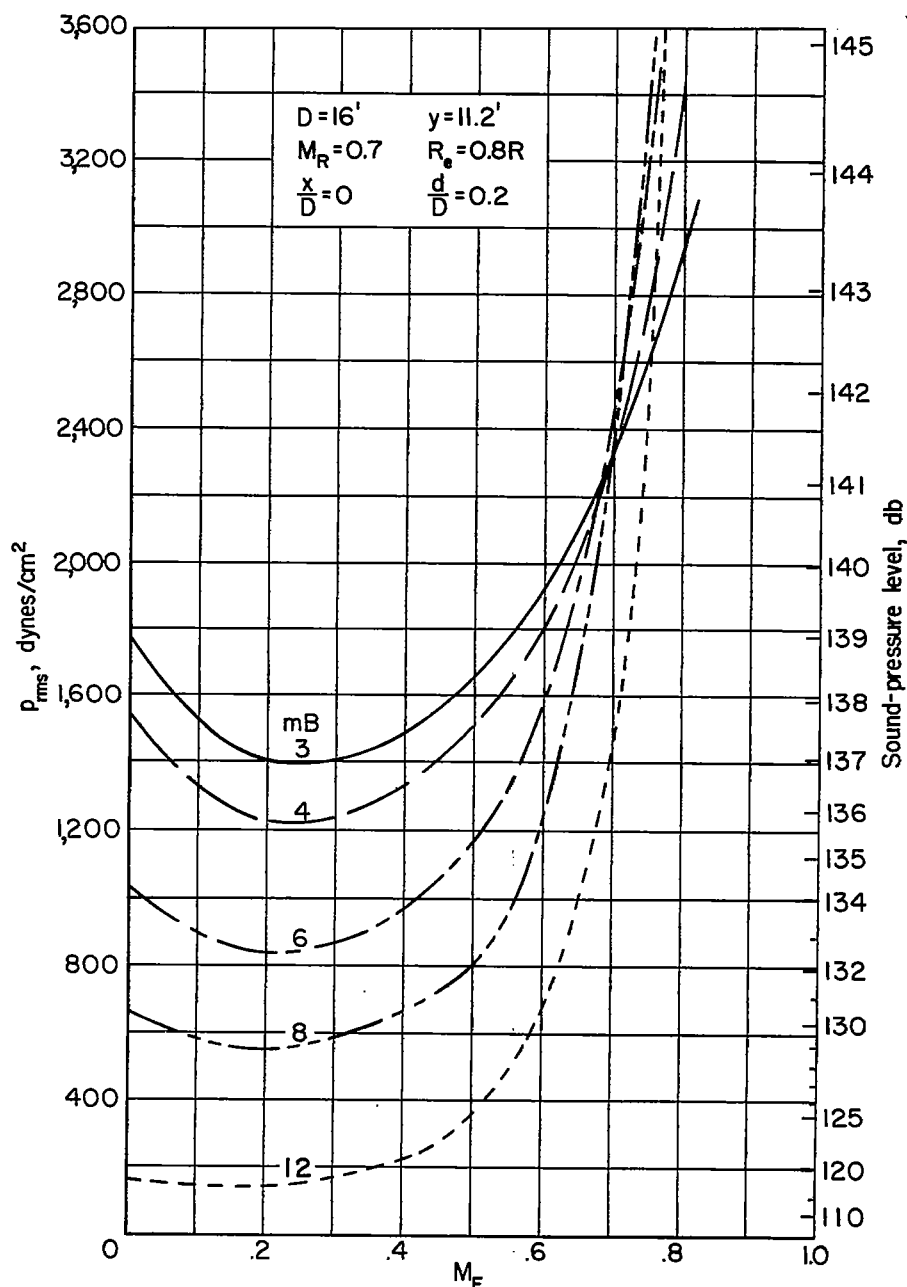
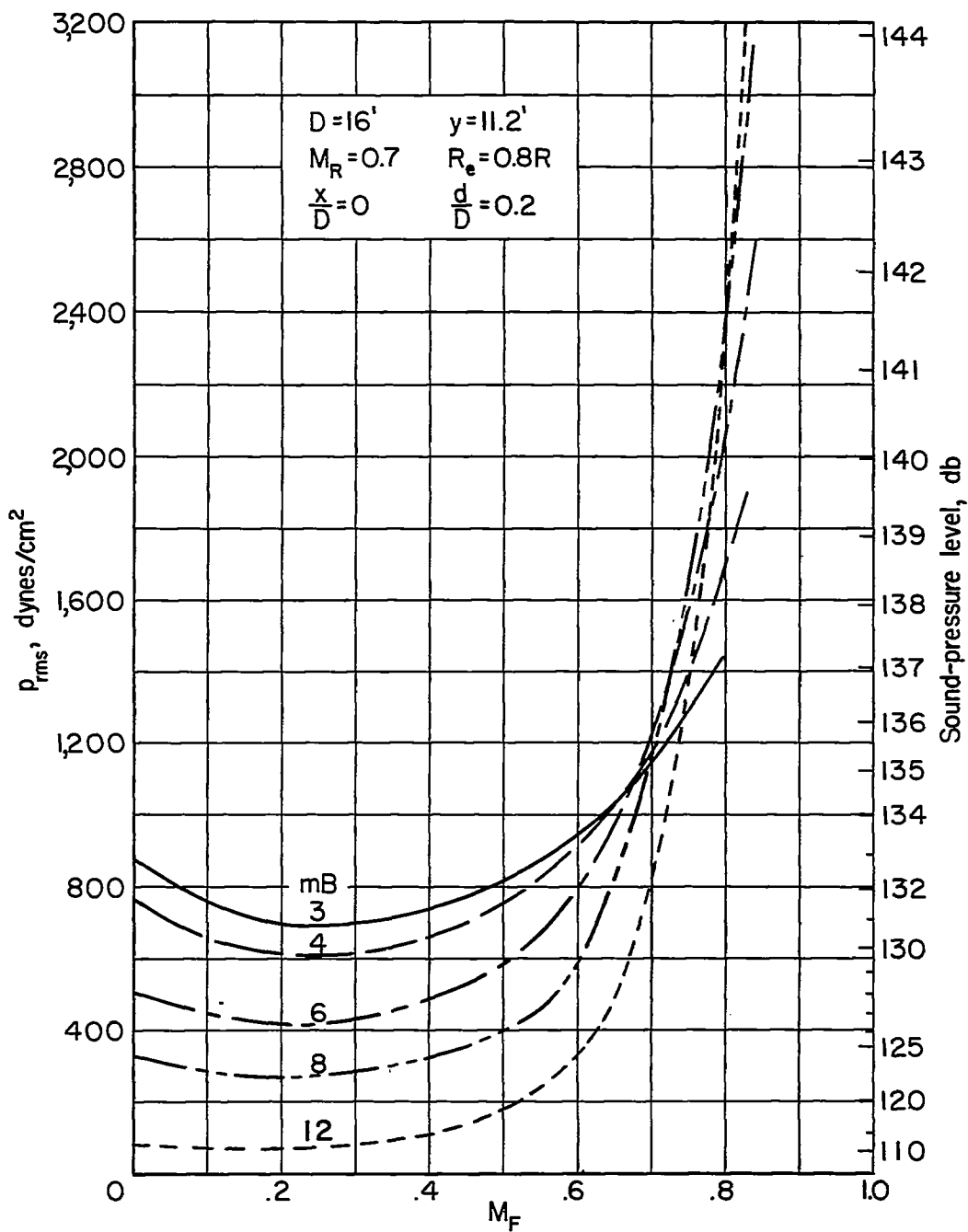


Figure 9.- Calculated root-mean-square pressures associated with first harmonic of a four-blade 16-foot-diameter propeller at a point 0.15D behind the plane of rotation as functions of flight Mach number for three different altitudes.



(a) Sea-level altitude.

Figure 10.- Calculated root-mean-square pressures for various values of mB in the plane of rotation for 16-foot-diameter propellers as functions of flight Mach number for two different altitudes.



(b) 35,000-foot altitude.

Figure 10.- Concluded.

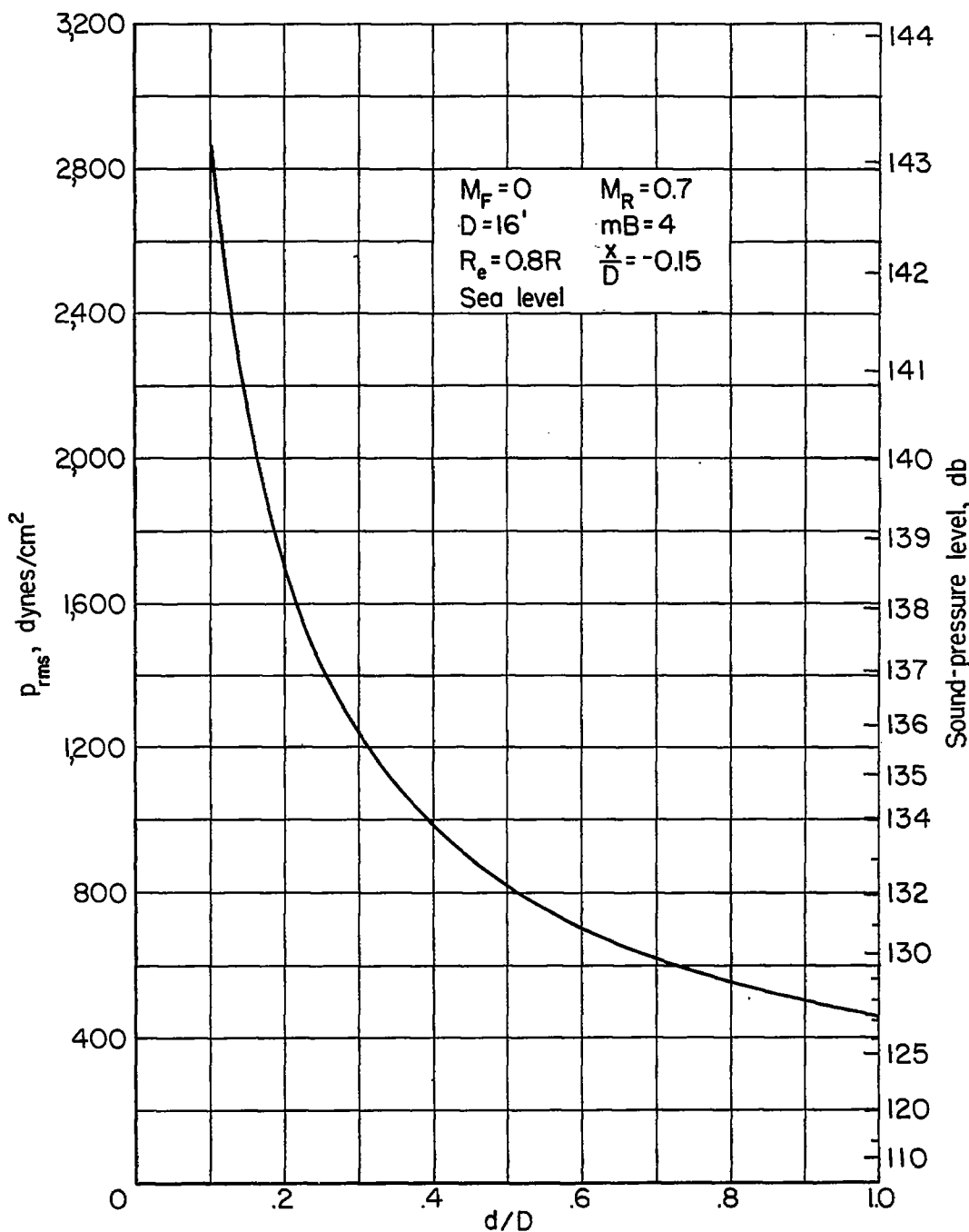


Figure 11.- Calculated root-mean-square pressure as a function of distance from propeller tip along a line 0.15D behind the plane of rotation for a four-blade 16-foot-diameter propeller operating at sea-level conditions.